Polyol-based soft hydrogels for biorecognition and tissue engineering applications

Inaugural-Dissertation

to obtain the academic degree

Doctor rerum naturalis (Dr. rer. nat.)

Submitted to the Department of Biology, Chemistry and Pharmacy of

Freie Universität Berlin

by

Rotsiniaina Randriantsilefisoa

Institut für Organische Chemie

Fachbereich Biologie, Chemie, Pharmazie

Freie Universität Berlin

2019

This Ph.D thesis was carried out under the supervision of Prof. Dr. Rainer Haag from October 2015 until December 2019 at the Institute of Biology, Chemistry and Pharmacy of the Freie Universität Berlin. The studies have been supported by the Focus Nanoscale Area and Helmholtz-Zentrum Geesthacht (HZG).

1. Reviewer: Prof. Dr. Rainer Haag, Freie Universität Berlin

2. Reviewer: Prof. Dr. Nan Ma, Helmholtz-Zentrum Geesthacht (HZG)

Day of Defense: 19.12.2019

Acknowledgement

I would like to thank Prof. Dr. Rainer Haag for the opportunity for this PhD thesis in his group. I would like to thank Prof. Dr. Nan Ma for her consent to be the second reviewer of this thesis.

I thank all former and present group members, including the subgroup members for their useful advice and support, also those who helped me to establish in the biology and chemistry labs.

I would like to express my gratitude to the collaborators in our group and other groups at FU, TU, HZG, and University of Potsdam and the group members that have helped in new interdisciplinary fields, in characterization techniques, social gatherings, and other organization.

I would like to thank the lab mates in the different floors of the buildings as well as the visitors who contributed to a nice work environment.

I also would like to thank Anja Stöshel and Cathleen Schlesener for the synthesis of polyglycerol amine. Gaby Hertel, Katharina Goltsche, and Cathleen Schlesener for taking care of chemical ordering and GPC measurements.

I would like to thank Pradip Dey and Badri Parshad for their help with the synthesis and useful discussions.

Many thanks to Yong Hou as well as Jianguang Zhang, Minjun Li, Jie, Yuanwei Pan, Sujuong, Yan Lee, and Paul Hillmann for their help in the work in the biolab.

I would like to acknowledge Dr. Wiebke Fischer, Jutta Hass, Eike Ziegler, and Lisa Hummel for dealing with all the paperwork and financial issues as well as taking care of ordering the chemicals. Further, I would like to thank the materials store staff for their friendliness.

I would like to thank Dr. Pamela Winchester for the careful language polishing of my manuscripts and this dissertation.

Many thanks to Uwe Schedler and his team for their collaboration and the opportunity to perform measurements at PolyAn GbmH, also for providing some materials and ideas.

Thanks to the service team of the core facility BioSupraMol for performing numerous NMR and MS measurements.

I would like to thank Ehsan Mohammadifar for MALDI-TOF measurements and nice discussions.

Thanks to José Luis Cuellar Camacho for AFM measurements and helpful discussions.

I express my gratitude to Michaël Kulka for SEM measurements and great discussions.

I am grateful to my family and friends for their support during all the years at FU Berlin.

I acknowledge the financial support of the Focus Nanoscale and Helmholtz-Zentrum Geesthacht (HZG).

Finally, I would like to thank any relevant people who helped with my thesis and have not been mentioned.

Content

List of Abbreviations

AFM	atomic force microscopy
AuNP	gold nanoparticle
CFS	colloidal force spectroscopy
dPG	dendritic polyglycerol
DMEM	Dulbecco's modified eagle medium
EDC	1-ethyl-3-(dimethylaminopropyl)carbodiimide
ELISA	enzyme-linked immunosorbent assay
GPa	gigapascal
GPC	gel permeation chromatography
GSH	L-glutathione-reduced
hMSC	human mesenchymal stem cell
IgG	immunoglobin G
kPa	kilopascal
LVER	linear viscoelastic region
MS	mass spectrometry
NHS	N-hydroxysuccinimide
NMR	nuclear magnetic resonance
PBS	phosphate buffer saline
PEG	poly(ethylene glycol)
RGD	arginine-glycine-aspartic acid
SPAAC	strain-promoted azide alkyne cycloaddition
SEM	scanning electron microscopy
TCPS	tissue culture polystyrene
TEM	transmission electron microscopy
UV	ultra-violet
Vis	visible
XPS	X-ray photoelectron spectroscopy
2D	two-dimensional
3D	three-dimensional

1 Introduction

An early diagnosis generally increases the chances of successful treatments. For these reasons, biosensing systems have started to emerge in the 1950s with Clark's first biosensor for oxygen quantification in blood that has led to the modern glucose sensor used by millions of diabetics.[1] Nowadays more technological inventions have been developed and have led to the next generation of biosensors: to only cite a few, portable assays, DNA chips, aptasensors, enzyme-based biosensors, immunosensors, lab-on-a-chips, microfluidics, medical wearables, and wireless sensor networks.[2] One common point of these technologies is their limitation to a two-dimensional detection (2D). In 2D detection systems, protein stability and conformation are at risk. Furthermore, they display a limited loading capacity, which leads to a lower sensitivity.[3] This makes the immobilization of molecules and biomolecules on the surface more of a challenging task because the stability of the biomolecules and the loading capacity influence the performance of the sensor.[4] As the integrity of the capture biomolecule is of a key importance in such application, an immobilization strategy that also takes the microenvironment of the capture molecule into account is critical.[3]

Three-dimensional (3D) matrices where biological entities are immobilized have gained in popularity in the past few years as extracellular matrices, biomolecules delivery systems, or in sensing applications.[5] The main advantage of hydrogels is their ability to provide a compatible environment for biological entities and surface chemistries that are adequate for proteins. Furthermore, their aqueous pores can host more biomolecules, without any conformational change in proteins. Their large surface area confers in principle a higher loading and binding capacity.[6] Therefore, hydrophilic matrices can provide a natural environment for immunological species but also for cells.[7]

Cell culture is now a standard method in the field of biology. Harvesting cells is needed in many fields of research from simple cytocompatibility tests to tissue engineering, cell-based therapy, and regenerative medicine.[8] For a few years now, these techniques are more and more in demand due to their high potential to cure diseases, to improve medical conditions, and to solve defects in human body. Especially, techniques that use human mesenchymal stem cells, multipotent cells that can differentiate into a large variety of cells have become increasingly developed.[9] Hydrogels are appealing as a material for building scaffolds since they have a structure comparable to extracellular matrices of tissues with a naturally hydrated state and can be tuned to give certain mechanical properties, biocompatibility, biodegradability, and morphology. They can be formed in mild conditions, they are relatively easy to deliver non-

invasively, which makes them an appropriate material to address issues in applications such as biological designs for engineering tissue replacements or for delivery.[10]

In this thesis, the advantages of three-dimensional systems for biomedical applications as well as their mechanical properties are explored. Hence, the formation of soft bioactive bio-orthogonal hydrogels is presented for three different applications: biosensing, bio-responsive systems, and tissue engineering. The aim is first to address the need for an alternative efficient immunoassay with a bioactive three-dimensional network. Another goal is to build a bioresponsive hydrogel system towards small molecules but especially towards a bigger biospecies. The third purpose is to develop a more proficient human mesenchymal stem cells culturing system. Therefore, all three concepts will be introduced in the background part of this work.

2 Background

2.1 Hydrogels

2.1.1 Definition

Hydrogels are hydrophilic polymer networks capable of swelling in the presence of water or any aqueous medium.[11] Natural hydrogels can be found in the body such as in the blood vessel, in the kidney, on the surface of the stomach, intestines, and lungs.[12] Synthetic hydrogels are achieved by simple reactions of one or several natural, synthetic, or hybrid monomers, polymers or crosslinker units. Since the pioneering work of Wichterle and Lim on the synthetic network based on poly-2-hydroxyethylmethacrylate (PHEMA) obtained via co-polymerization of triethylene glycol monomethacrylate with triethylene glycol dimethacrylate, different varieties of hydrogels have been synthesized and used for biomedical applications.[13] A classification of hydrogels is based on their preparatory routes being either chemical or physical/self-assembled crosslinking and further based on their physical properties as described in Figure 1.[14]

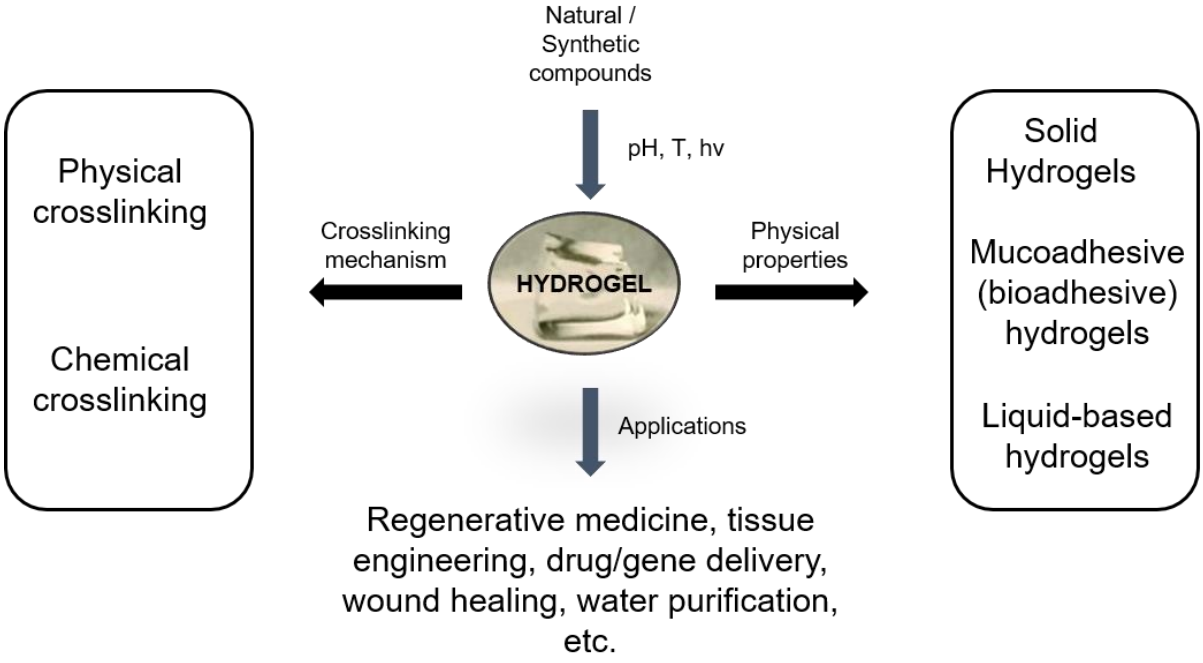

Figure 1. Classification of hydrogels and their applications. Inspired from ref. [14a]. Copyright © 2017 Elsevier.

2.1.2 Chemistry of Hydrogel Formation

Hydrogels are hydrophilic polymer networks. Therefore, any strategy to obtain a crosslinked matrix can be used to obtain such material. Hydrophilicity is enhanced by water-solubilizing functional groups (-OH, -COOH, -$CONH_2$, -SO_3H).[15] Synthesis can be performed in solution, gas phase, emulsion, suspension, by plasma, or bulk polymerization.[16] Many strategies are readily available in the literature and some typical routes are being reported below with a special focus on biomedical applications. For this field, reactions should occur at mild and aqueous conditions without any toxic side products or high temperature.[17]

Free Radical Polymerization Between Monomer and Cross-Linking Agent

Free radical polymerization is among common methods utilized to generate a three-dimensional crosslinked structure over other methods of hydrogel formation due to the several advantages that they offer. Free radical polymerization is characterized by a high reactivity and a large variety of functional groups as well as the possibility of reaction in aqueous conditions. This category can also be classified in copolymerization, homopolymerization, and multipolymer- interpenetrating polymeric hydrogels.[18]

Homopolymeric hydrogels are generated by a unique monomer, in the presence of an initiator (as an example, 2,2′-azo-bisisobutyronitrile (AIBN)) and a chemical crosslinker (e.g., an acrylamide free radical).[19] For example, F. Liu et al. have used N,N′-methylenebis(acrylamide) as a chemical crosslinker to form the first example of hydrogel networks showing reversible positive swelling behavior in water and electrolyte solutions.[20]

Copolymerization involves at least two different monomers with at least one hydrophilic monomer. The resulting polymer chains are further classified as random, block, or alternating copolymers.[21] For example, M. Zhou et al. have produced a pH-temperature dually sensitive hydrogels for drug release applications with the copolymer poly[N,N-dimethylaminoethyl methacrylate-co-poly(poly(ethylene glycol) methyl ether methacrylate)(poly(DMAEMA-co-MPEGMA)).[22]

Interpenetrating polymer networks (IPN) or semi-interpenetration polymer networks (Semi-IPN) are hydrogels composed of two independently crosslinked hydrogels or one crosslinked hydrogel with one non-crosslinked hydrogel, respectively.[23] These types of networks are more and more used in the biomedical field as they offer several properties in

only one system: reinforced mechanical properties, improved stimuli responsiveness, and tuned physical properties.[24] This technique, for instance, has allowed the fabrication of dually responsive hydrogels by mixing pectin and poly(acrylamide-co-acrylamidoglycolic acid).[25]

Synthesis in solution or suspension polymerization are the most frequently used methods for free radical polymerizations, where solution polymerization lead to bulk and variously shaped hydrogels, while suspension gives round and spherically shaped hydrogels.[26]

Chemical Reaction of Complementary Groups

Direct reactions between functional complementary groups can be utilized to form hydrogels. A few examples of reactions for this type of hydrogel formation are reported.

Click reactions of alkyne, cyclooctyne, or oxanorbornadiene with azide, Cu-catalyzed or not, consists in a cycloaddition of azide with alkyne or cyclooctyne to form a triazole ring, with a strain-promoted reaction (copper-free reaction) in the case of the cyclooctyne.[27] A specific example is a reaction of difluorinated cyclooctyne with azide, where the reaction is facilitated by the ring strain and the electron-withdrawing difluoride.[28] Click reactions have a high efficiency and high selectivity, without any formation of by-products. They also occur in aqueous conditions and an add-on is the bioorthogonal nature of the reaction, which prevents the formed network from interacting with biological species making them ideal for biomedical applications. As an example, C. A. DeForest et al. have reported a peptide-functionalized-hydrogel with tunable mechanical properties for cell culture using difluorinated cyclooctyne and azide click strategy.[29]

Michael addition (reactions of maleimide, vinyl sulfone, acrylate, methacrylate with thiol) is a 1,4-addition of nucleophiles to α,β-unsaturated ketones or esters, a reaction with high efficiency that occurs in aqueous conditions.[30] The advantage of Michael addition is the absence of side products. Typically, nucleophiles are multi-terminated macromolecules with thiol or amine groups, whereas electrophiles are alkene functional groups with adjacent groups having electron-withdrawing capability. Surfactants can be used to enhance the kinetics of the reaction, depending on the electron deficiency of the alkene.[30]

Another method for the synthesis of hydrogels is a Schiff-based formation (reaction of aldehyde with amine, hydroxylamine, or hydrazide to form an imine, hydrazine, or oxime linkage).[31] The reaction rate can be tuned with the pH and one characteristic of this reaction

is that aldehyde-containing compounds can react with the amine of biological species for biomedical applications.[32] For example, T. Hozumi et al. have proposed an injectable degradable hydrogel using gelatin and hyaluronic acid. Hydrazine linkage is labile and reversible by hydrolysis, and the stability of an imine is quite low compared to, for example, an oxime linkage. The stability of the bonds will determine the stability of the hydrogels. There is a possibility to reinforce the hydrazone linkage by distributing the charge around the hydrazine moiety.[33]

Furthermore, thiol-ene/yne coupling (reaction of alkene/yne, norbornene with thiol) is often used in hydrogel formation.[34] The initiation of the radicals can be done by various methods, namely, thermally, photochemically, or by oxidation reduction.[35]

Another main strategy used to form hydrogels for biomedical applications are Diels Alder reactions (reaction of norbornene, trans-cyclooctene with tetrazine, or reaction of furan with maleimide). This type of reaction is rapid, highly selective, effective, and forms a robust linkage.[36] For instance, L. J. Smith et al. have synthetized hydrogels by Diels-Alder click reaction for cell encapsulation applications.[37]

Moreover, disulphide formation (reaction of thiol with another thiol) is used as well.[38] They are obtained by simple oxidation of thiol groups, but the main disadvantage of the method is a low stability of the hydrogels in the presence of reducing agents or certain enzymes.[39]

Finally, epoxide reactions (reaction of epoxide, diepoxide with amine or thiol) can be utilized. This type of reaction is insensitive to oxygen conditions and the epoxy species as electrophiles react with nucleophiles such as thiol groups, carboxylic acids, or amines.[40]

2.1.3 Hydrogel Properties

Swelling

The swelling property of a hydrogel is influenced by different parameters: the network density, the solvent's nature and the molecular weight between two crosslinking points.[41] Different osmotic pressure present in the hydrogel and in the aqueous environment results in the swelling of hydrogels. The response of the polymeric network is an elastic stress during the stretching of the polymer chains.[42] Because water is considered as a plasticizer in a hydrophilic polymer network, the swelling can be considered as a rubbery state. The Flory-Rehner equation

therefore describes it with the equilibrium status of the swollen state characterized by the Gibbs free energy, given by two components: one characterizes the thermodynamic force of mixing, which favors swelling, and is balanced by the stored force by the polymer chains that hinders swelling, as described by Equation (1), where ΔG_{mixing} (entropic component) results from mixing of, e.g., water and polymers, while $\Delta G_{elastic}$ (enthalpic component) is the result of the extending polymer chains in the presence of water molecules.[43]

$$\textbf{(1)}\quad \Delta G_{total} = \Delta G_{elastic} + \Delta G_{mixing}$$

At the beginning of the swelling, $\Delta G_{mixing} << 0$, $\Delta G_{elastic} > 0$, and $\Delta G_{total} > 0$. During the swelling, both components increase until $|\Delta G_{mixing}| = |\Delta G_{elastic}|$, $\Delta G_{total} = 0$, at equilibrium, with the chemical potential inside the gel being the same as outside the gel.

The swelling can be calculated and given by the degree of swelling, also called swelling ratio, given by Q in Equation (2):

$$\textbf{(2)}\quad \boldsymbol{Q} = \frac{\boldsymbol{w_{wet} - w_{dry}}}{\boldsymbol{w_{dry}}}$$

w_{wet} being the weight of the hydrogel in swollen state and w_{dry} being the weight of the hydrogel in dry state.

Mesh Size

The diffusion properties in a hydrogel are due to the spacing in a hydrogel also characterized as "pores."[6] According to the pore size, the hydrogels are either called "macroporous", "microporous", or "non-porous". The mesh size, characteristic of the pore, is given by the parameter ξ defined by the linear distance between two crosslinks (Equation 8). The mesh size ξ is given from the rubber elastic theory using the following equations:[44]

The shear stress τ is given by the Equation (3).

$$\textbf{(3)}\quad \boldsymbol{\tau = \rho \frac{RT}{\overline{Mc}} \left(1 - \frac{2\overline{M_c}}{\overline{Mn}}\right) \left(\alpha - \frac{1}{\alpha^2}\right) \left(\frac{\nu_{2,s}}{\nu_{2,r}}\right)^{1/3}}$$

ρ: polymer density, $\overline{\boldsymbol{Mc}}$: molecular weight between crosslinks, $\overline{\boldsymbol{Mn}}$: average monomers molecular weight, $\nu_{2,s}$: polymer volume fraction in the swollen state, $\nu_{2,r}$ the polymer volume fraction in the relaxed state, α the elongation ratio, T: the absolute temperature and R: the universal gas constant,. The volume fractions are obtained with Equation (4):

$$(4)\ \boldsymbol{\nu_{2,s} = \frac{1}{Q_s}\ ;\ \nu_{2,r} = \frac{1}{Q_r}}$$

with Q_s and Q_r the respective swelling ratios. The shear modulus G is given by Equation (5):

$$(5)\ \boldsymbol{\tau = G\left(\alpha - \frac{1}{\alpha^2}\right)}$$

Combining Equation (3) and (5) gives Equation (6):

$$(6)\ \boldsymbol{G = \frac{\rho RT}{\overline{M_C}}\left(1 - \frac{2\overline{M_C}}{\overline{Mn}}\right)\left(\frac{\nu_{2,s}}{\nu_{2,r}}\right)^{\frac{1}{3}}}$$

with (7):

$$(7)\ \boldsymbol{\frac{G_s}{G_r} = \frac{RT\rho_x Q_s^{-\frac{1}{3}}}{RT\rho_x Q_r^{-\frac{1}{3}}} = \frac{Q_s^{-\frac{1}{3}}}{Q_r^{-\frac{1}{3}}}}$$

G_s and G_r being the equilibrium shear modulus and relaxed shear modulus, respectively.

Finally, the mesh size is given by Equation (8):

$$(8)\ \boldsymbol{\xi = \nu_{2,s}^{-\frac{1}{3}} l\sqrt{\frac{2C_n\overline{M_C}}{M_r}}}$$

where l is the bond length along the polymer backbone, C_n the Flory characteristic ratio, M_r the molecular weight of the repeating unit.

Mechanical Properties

Mechanical properties are of a tremendous importance in biomedical applications.[45] The mechanical characterization of the biomaterial is essential to predict the behavior of biological entities at the interface.[46] For instance, mechanical properties need to be tuned to get optimal materials for wound dressing applications and matrices for drug delivery, tissue repair, tissue replacement, and biosensing.[47] As an example, in drug delivery, the hydrogels should be such that it maintains its stability during the process of delivery for a determined period of time before releasing the therapeutic entity at the targeted region. Getting the desired mechanical property is achieved by modifying the crosslinking density, the number of hydrogen bonding or the molecular weight.[48] Mechanical properties of hydrogels are determined in the linear viscoelastic range, giving the Young's Modulus, and based on Flory's theory, the crosslinking density and the average polymeric mesh size can be obtained.[49]

Biocompatible Properties

Biocompatibility is the property of not producing a toxic or an immune response when exposed to the body or a body part. This represents a key feature for materials used in biomedical applications.[50] This property is mainly influenced by the nature of the molecules in presence.[51] To prove the biocompatibility of a material, *in vitro* cell culture tests are usually performed, also known as cytotoxicity tests.[52] Most issues of hydrogels are associated with toxicity due to unreacted monomers, oligomers, or initiators leaching out of the system.[53]

2.2 Polyethylene Glycol for Biomedical Applications

Polyethylene glycol (PEG) is a hydrophilic neutral polyether available in a variety of molecular weights.[54] This molecule has been popular among the biomedical community due to a broad range of advantages.[55] PEGs are inert to cells and non-toxic to active proteins.[56] They can be chemically modified to bind other molecules without having any effect on their chemistry. In addition, their solubility and size are tunable.[56] They can be anchored on surfaces and have been utilized in purification of proteins and nucleic acids. In combination with dextran, PEGs form a two-phase system in buffer usable for purification of biological species.[57] Furthermore, previous findings have suggested that PEGs interact with cell membranes and give cell fusion which is also an interesting feature in biotechnology.[58] PEGs have also been utilized to stabilize serums by conjugation of PEGs with proteins.[59] Finally, when PEGs alone are attached on a surface, no protein adsorption is observed, giving the anti-fouling property to the surface.[60] Since these findings, PEG has become the benchmark for anti-fouling material. Hetero- and homo-functional PEG derivatives are suitable crosslinking agents or spacers, where monofunctional PEG prevents bridging reactions.[55] Multi-armed PEG derivatives are commonly used in the formation of hydrogels.[61] Applications for PEG encompass drug release, development of medical devices, regenerative medicine, cell culture, wound dressings, targeted diagnostics, and many others.[62] Though, immunological recognition of PEG upon several exposures can represent a major drawback for some *in vivo* applications.

2.3 Dendritic Polyglycerol for Biomedical Applications

The control at the bio-interface of materials is crucial especially in biomedical applications.[63] For this aim, coatings are often used on devices to prevent unspecific interaction with the

biological surroundings but simultaneously allowing specific biological interactions.[64] From many studies, polyethylene glycol-based material became a feature standard as anti-fouling material (PEG as linear polyols). However, some drawbacks such as biocompatibility and a poor number of functionalities remain. In the same category of polyols, hyperbranched (hPG) or dendritic polyglycerols (dPG) (Figure 2) represent good candidates as they offer a broader range of functionalization due to the several hydroxyl groups exposed at the end of the branches.[65] dPG is prepared by ring-opening, anionic, multi-branching polymerization, obtained with a narrow polydispersity.[66] In addition to being highly biocompatible, they also have no interaction with proteins, which allows a strong stability of immobilized proteins in dPG-based matrices. This high biocompatibility of PG has allowed one to build different systems for diverse applications in the biomedical applications, for example, in pharmaceuticals, additives, tissue engineering, medical devices, drug delivery, to cite only a few.[67]

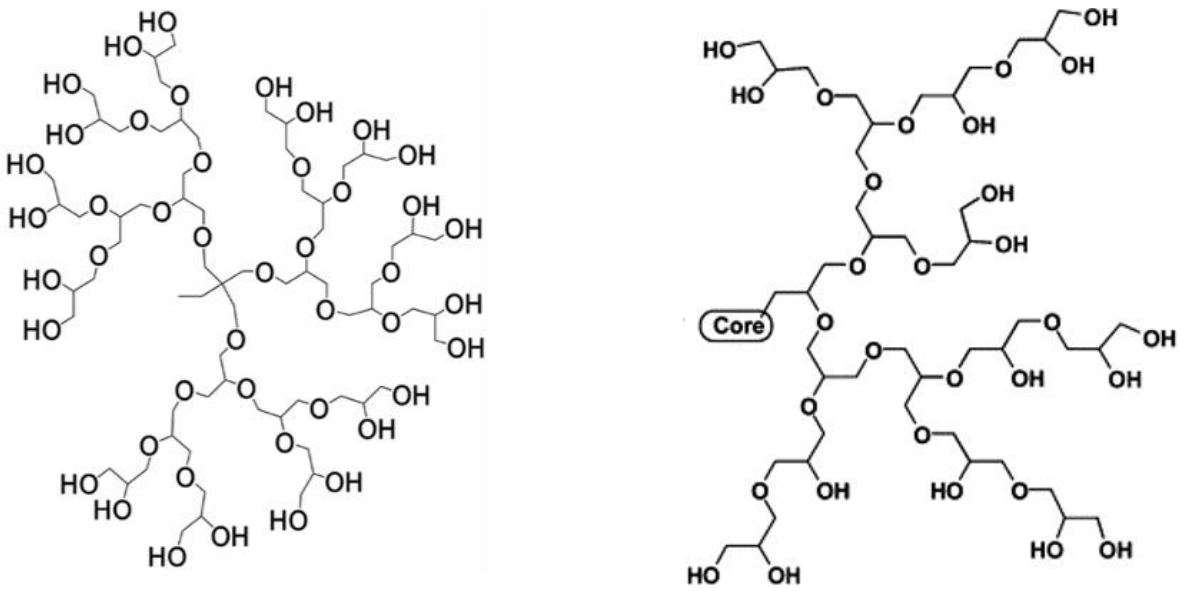

Figure 2. dPG (left) and hPG (right) molecules. Modified reprint with permission from ref. [67a] Copyright © 2009 Wiley-VCH Verlag GmbH & Co. KGaA.

2.4 Other Polymers for Biomedical Applications

Biomaterials can be formed from natural or synthetic polymers.[68] Natural polymers are divided into three categories: proteins (silk, collagen, fibrin), polysaccharides (hyaluronic acid, alginate, and chitosan), and polynucleotides (DNA and RNA).[69] For the most common

synthetic polymers, polyesters, for example, poly(lactic acid), poly(glycolic acid) and poly(lactic-co-glycolic acid) or polycaprolactone are used to form hydrogels, other examples are polyurethanes.[70]

2.5 Click Reactions in Materials Science

The goal of material scientists has been so far to build a final material derived from reactions as simple as possible as well as fully efficient. The aim is to develop performant devices or structures. They are looking for specific mechanical, physical, and morphological behavior, for instance, stiffness, thermo-responsiveness, and roughness and, at the same time, (bio)chemical properties such as surface energy, chemical functionalities, biocompatibility, and biodegradability.[71] Designing a chemical strategy has been motivated by the need to get these above-mentioned performances. This is how the concept of "click" reaction was first introduced in 2002 by Sharpless et al.[72] Their argument was the possibility to go through a route of several simple reactions to get the same natural products obtained via synthesis involving many complicated purification steps, protecting groups, and many reactions steps.[73] These reactions are orthogonal, simple to purify and affords high yields.[71] This toolbox now also allows reversible click reactions.[74] Common click reactions are reviewed below (described in Figure 3).

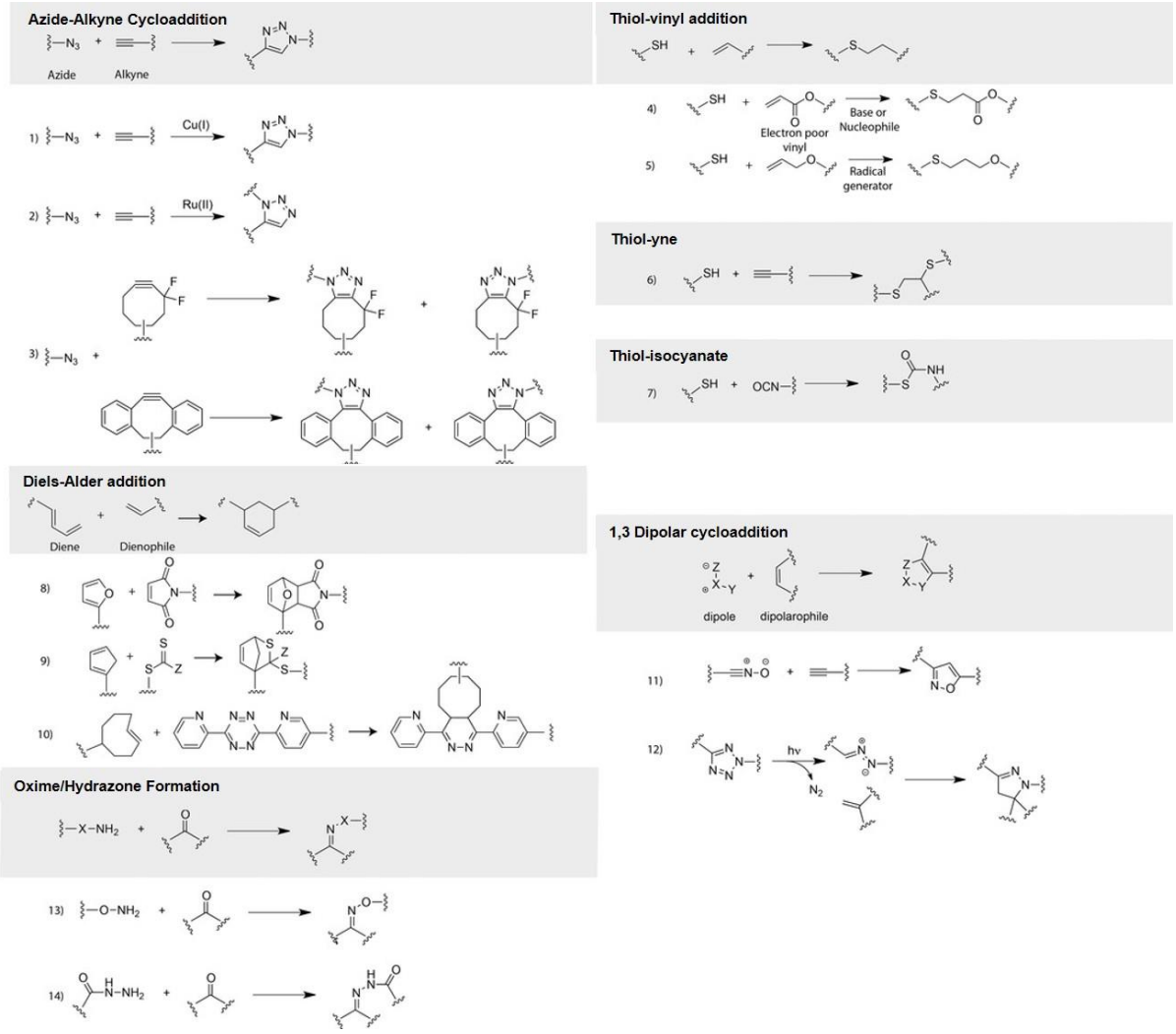

Figure 3. Summary of the common click reactions used for biomedical applications. Modified reprint with permission from ref. [71] Copyright © 2014 Wiley-VCH Verlag GmbH & Co. KGaA.

Azide-Alkyne Cycloaddition

Click reaction of azide to alkyne has started with a [3+2] cycloaddition between both species to yield 1,2,3-triazole at high temperatures. The drawback of this reaction is that it gives side products affording both 1,4 and 1,5 regioisomers. To optimize the reaction, instead of using heat, Cu(I) was introduced to catalyze the reaction and this was called CuAAC. The reaction is selective, yielding only the 1,4-regioisomer. However, Cu(I) is thermodynamically unstable, affording Cu(II) and Cu(0), especially Cu(II) by oxidation. To circumvent the issue, Cu(I) is generated from Cu(II) by using a reducing agent (ascorbate). Another catalyst can be ruthenium (II) but yielding the 1,5-disubstitued 1,2,3 triazole regioisomer. However, Cu is cytotoxic and

therefore ring strain strategy has emerged to tackle the use of Cu. As an example, fluorosubstituents of cyclooctyne combines the ring strain and electron withdrawing property and this allows a rapid reaction in the absence of heat and any catalyst. Another strategy is to incorporate sp^2 centers to the cyclooctyne ring with dibenzocyclooctyne, which has the same reaction rate as with the fluorinated cyclooctyne. These reactions are irreversible and yield chemically inert and thermally stable products in normal conditions but reversible under ultrasonification.[72]

Thiol-Ene/Yne/Isocyanate Click Reaction

Thiol-ene reactions are the most common click reaction in the family of thiol reactions. Two types of reactions are possible: a radical mechanism or a nucleophile-mediated mechanism. In the first option, the reaction is initiated by the formation of radicals by light or higher temperature. Then, a thiyl radical is added to an alkene. A carbon-centered radical is subsequently produced. A hydrogen is abstracted by the radical from a thiol compound yielding a thioyl radical and a thioether. This is optimal when using an electron-rich alkene group (allyl ether or simple alkene). This reaction is water stable as well as oxygen inert due to the peroxy radical's ability to abstract a hydrogen from a thiol but in the condition that the concentrations of initiator, oxygen, and any source of chain transfer are optimized (solvent, initiator concentration), uniform light intensity, and a low level of oxygen). The same is applicable to a thiol-yne reaction where each alkyne reacts with two thiols yielding a dithioether. However, undesired products appear due to radical-radical coupling reactions during the process. Besides, nucleophile-mediated click reactions involve thiols or electron-poor vinyl groups (acrylates, vinyl sulfones, maleimides). This reaction generates a carbon-centered anion that represents the strong base and produces a thiolated anion, which then initiates the thiol-Michael addition catalytic cycle that does not yield any side product. Thiol-isocyanate is also another type of click reaction with high yield producing thio-urea products.[71, 75]

Diels-Alder Cycloaddition

Diels Alder is a robust pathway that uses a diene and a dienophile to form a cyclohexene derivative and this reaction is thermally reversible. Inverse electron demand Diels-Alder

consists in a reaction between a strained alkene or alkyne and a tetrazine to yield a dihydropyridazine or pyridazine.[76]

Tetrazole Cycloaddition and Nitrile Oxide Cycloaddition

Another example of 1,3-dipolar cycloaddition reaction is between a 2,5-diaryl tetrazole and an alkene. Upon irradiation, the 2,5-diaryl tetrazole releases a N_2 molecule to yield a nitrile imine, which then reacts with the alkene.[71]

Oxime/Hydrazone Formation

The chemoselective oxime-hydrazone formation reaction can be used with functional groups of biomolecules. The advantage is the mild and rapid approach, but the stability of the linkage is relatively limited. Aldehydes or ketones and nucleophilic amines give a reversible imine bond by condensation reaction. The reactivity of aldehydes is more important than ketones because of steric effects. For example, the reaction between a hydroxylamine and hydrazide affords an oxime and hydrazine products.[73]

2.6 Antibody-Antigen

2.6.1 Antibodies

Antibodies (Ab) also known as immunoglobulin (Ig) are glycoproteins in Y-shaped with a large molecular weight. They are mainly produced by B-cells of the immune system. An Ab recognizes a unique molecule of a pathogen, called an antigen, via the fragment binding antigen variable region (Fab). Each part of the Y shape contains a paratope, which is specific to one epitope of an antigen (Figure 4). This complex formation may hinder the biological process that might cause disease. It might also activate macrophages to engulf and destroy the pathogen. The communication of the Ab with the rest of the immune system is mediated by the Fc region at the base of the Y shape, since it contains a glycosylation site involved in the communication process. Antibodies can be either soluble, destined to be secreted in the blood plasma, or attached to the surface of a B-cell which refers to a B-cell receptor (BCR). These will be involved in future recognition, also part of the immune memory process. [77]

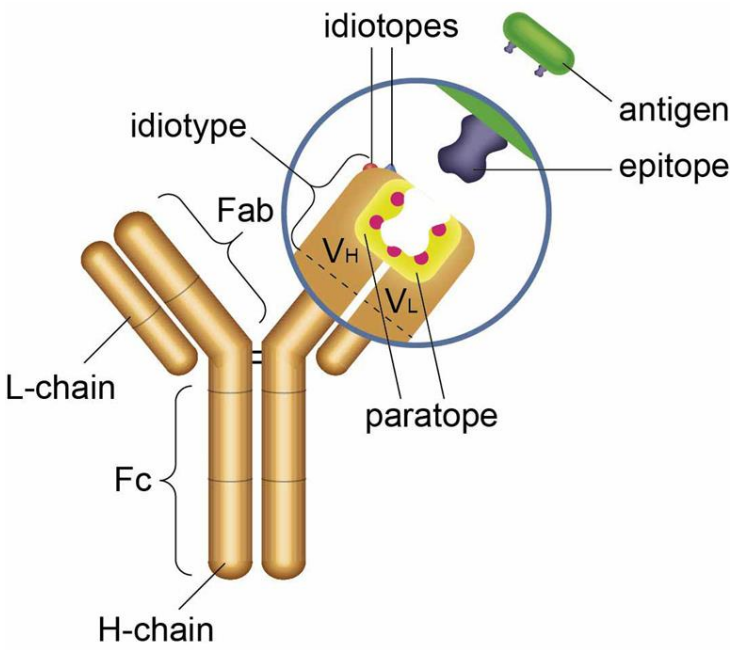

Figure 4. Schematic representation of an antibody and its interaction with an antigen.

The structure of an Ab can be divided into two components, two large heavy chains and two small light chains (Figure 4). The Fc region of antibodies are divided in five types, which allows the classification of Ab into five isotopes. Different isotopes have different roles and direct in different ways the appropriate immune response for different types of foreign bodies. As an example, the IgE isotope is responsible for the recognition of allergens that triggers a histamine release and mast cells' degranulation. Although Abs of different subclasses have similar structures, the small regions have highly variable structures. This region is called hypervariable region. Each variant can bind a different antigen and the diversity allows recognition of a myriad of antigens followed by a mutation in the antibody gene, which then creates more diversity. Ab also can change one type of the heavy chain Fc fragment to another, creating a different isotope which allows the Abs to be used by different receptors in the immune system.[78]

2.6.2 Peptides

The synthesis of peptides is done by condensation reaction of the amine group with the carboxyl group of each amino acid. Strategies such as protecting groups are often useful to prevent side reactions with the numerous amino acid on the side chains present. Typically, the synthesis starts at the carboxyl end of the amino acid. The chemical synthesis of peptides is

done by solid-phase technique (SPPS) in research and development but, in large scale industry, solution-phase synthesis is more useful.[79] SPPS consists in a rapid assembly of amino acids on an insoluble porous support. It is one repeated cycle of deprotection and coupling reactions. The support (gel-type, surface-type or composites) is usually a small, polymeric resin beads that are functionalized with reactive groups (amines, hydroxyl groups). These reactive groups covalently attach the peptide chain to the support. Washing and filtration removes excess reagent or side products. Protection (Boc (acid-labile) and Fmoc (base-labile)) at the N-terminus of each amino-acid that is going to be coupled to the peptide. After each reaction, the resin is rinsed. The amino acid is attached to the resin. After that, the amine is deprotected. Subsequently the deprotected amine is attached to the free acid of the other amino acid. This is repeated until the desired sequence of the peptide is obtained. The last step consists in cleaving the peptide from the support and simultaneously removing the protecting groups with strong acids (trifluoroacetic acid or a nucleophile). Precipitation of the crude product is perfomed from with a non-polar solvent such as diethyl ether to remove any byproducts. The purification of the peptide is done by HPLC. The longer the peptide is the more byproducts must be purified, which makes the process more challenging. Alternatively, continuous chromatography processes could be used. SPPS is limited to low yields and the synthesis process is sequence-dependent, making some peptides difficult to make.[80]

2.6.3 Viruses

Viruses are pathogens that can only replicate inside living cells. They are infectious to all kind of living beings, from animals, bacteria to plants.[81] There are five thousand viruses described and known but in reality there are millions of types. Therefore, the virus is the most versatile form and numerous of biological entity. Viruses are called virions or virion particles when outside a cell and exist as particles. They consist in a genetic material (DNA or RNA) surrounded by a protein coat (capsid), which protects the genetic part, and for some virions, an envelope of lipids around the capsid. They are shaped in helical or icosahedral but more complex forms can be seen in nature. Their size varies for most of the known ones from 20 to 300 nm.[82]

Influenza virus

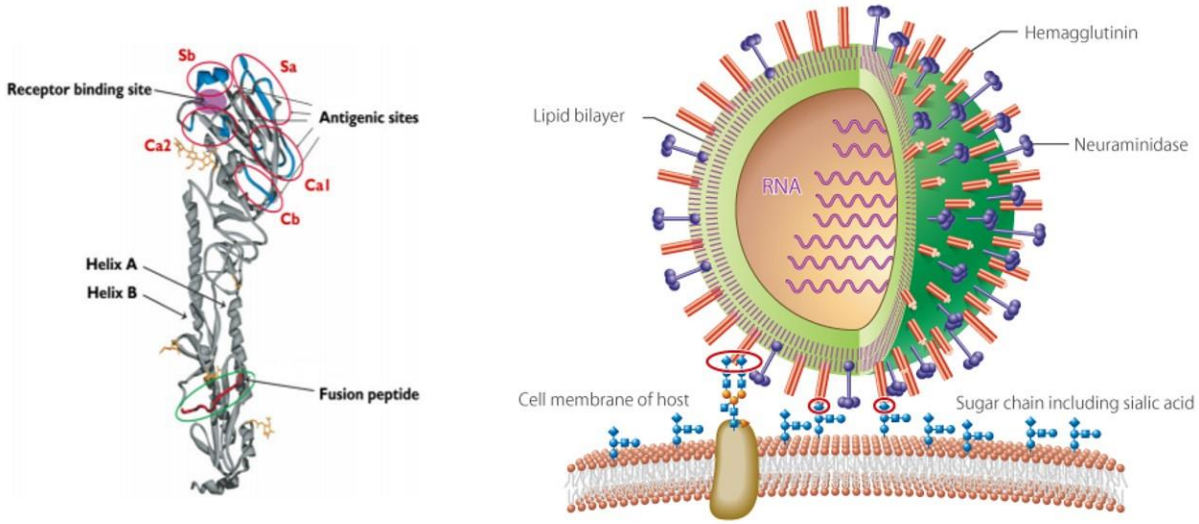

Figure 5. On the left, ribbon diagram of an uncleaved hemagglutinin monomer of a H1N1 Influenza A virus. The head is made-up of sialic acid receptor-binding site, surrounded by five predicted antigenic sites (Sa, Sb, Ca1, Ca2, Cb). The stem consists of helices A and B and the fusion peptide. On the right, schematic representation of the virus and cell wall interaction during infection. Copyright © 2008 Elsevier Ltd. Copyright © Division of Avanced Education in Sciences, Komaba Organization for Educational Excellence, College of Arts and Sciences, University of Tokyo.

The morphology of the envelope of the virus can be spherical or filamentous and the virus is generally ellipsoidal with a size around 80 to 120 nm or if filamentous, 80 to 120 nm in diameter and up to 20 µm in length.[83] The main glycoproteins, hemagglutinin (HA), are irregularly distributed with neuraminidase (NA), with a ratio HA to NA of around 5 to 1. HA and NA play a role in the entering and release of the virus in and out the cells to be infected. NA is an enzyme involved in the release of the virus from infected cells. NA hydrolyzes the ethers or glycosidic linkages between the sialic acid and the glycan present on the cell surface, normally galactose or N-acetylgalactosamine). The virus enters the epithelial cells in the lung and in the throat by endocytosis. HA is a lectin that serves as mediator of the binding event between the virus and the target cell and the viral genome entry into the cell through binding to sialic acids (Figure 5).[84]

2.7 Antibody-Peptide-Based Biosensors (2D and 3D)

2.7.1 Definition and General Information

The detection of Abs to prevent infectious diseases has been used for many years now. For example, bacteria-specific Abs (IgG and IgM isotopes) have been used to detect bacterial infections in serum of patients.[85] This technique is very useful in the case of viral infections such as hepatitis, rabies, herpes virus, and others.[86] The same applies for parasites that lead to diseases such as malaria and toxoplasma-allergen specific IgEs.[87] The method also serves to observe the success of immune therapy, with, e.g., venoms from several animal species. Another type of disease relevant for antibodies detection are auto-immune diseases, where the measurement of Abs shows abnormalities and serves as prediction and diagnosis tools. An example of such disease, where the immune system recognizes its own healthy tissues and organs as pathogens, is Hashimoto's thyroiditis disease with circulating Abs against thyroglobulin and myasthenia gravis with auto-Abs against acetylcholine receptor. Other examples are rheumatoid arthritis, scleroderma, affecting the joints, the skin, involving antibodies against antigens (DNA, RNA, or histones).[88]

The current clinically used antibody detection methods are mainly immunoprecipitation assay, immunocytometry, immunoblotting, and immunosorbent assays.

Immunoprecipitation Assays

Immunoprecipitation assay is an *in vitro* assay for a semi-quantification of antibodies. The principle of the method is the addition of the antigen to the Ab. As a result, this forms a complex aggregate that precipitates and is detected through a nephelometer (instrument that measures the concentration of suspended particulates in a liquid or gas). Another variation of this method is called hemagglutination assay where the Abs are identified by red blood cell antigens.[89]

Immunocytometry

Immunocytometry is a detection method of the complex antigen/Ab in tissues. The tissues are isolated, fixed, or frozen. They are cut into slices before immobilization on a slide. They are incubated with the Ab solution for the detection of the antigen in the tissue. In a direct assay, fluorescently labelled primary antibodies are directly detected by fluorescence microscopy. In

an indirect assay, the tissue is further incubated with a secondary antibody which have the fluorescent species while the primary antibody is non fluorescent.[90]

Immunoblotting

In immunoblotting or dot-blot technique, the Ab-antigen complex reacts on a solid phase (nitrocellulose membranes). The antigens are applied on the membrane and subsequently dried. After that, to avoid non-specific adsorption, it is necessary to add gelatin, ovalbumin, or milk proteins (blocking step). The membrane is then incubated with different concentrations of the serum containing Abs, which are conjugated with an enzyme. A substrate is then added, which is converted by the enzyme attached, yielding a color or a light-emitting spot. The concentration is proportional to the intensity of the spots.[91]

Immunosorbent Assays

IgG and IgE are often assessed by immunosorbent assay (IA). The concept is very similar to immunoblotting. Yet this technique can quantify the number of antibodies better. The antigen is attached to an inert substrate (vial, well plate, paper disc). The serum of a patient is incubated with the antigen carrying substrate allowing the binding Abs-antigen. After removing the excess serum, a secondary antibody is added. This forms a complex with the previous one. After another washing, a standard curve with different known concentrations of antigens will allow it to quantify them by comparing the signal with the one of the standard curves permitting the quantification of the antibodies. One of the most used one is the so-called ELISA (enzyme-linked immunosorbent assay).[92]

The common point of these methods is to detect in a 2D fashion, where either the molecule of recognition is immobilized on a plain surface or in solution, where antibody and antigen form a complex that is subsequently detected. In both cases, the stability of the proteins is at risk, where a conformational change can occur, or a loss of function and denaturation.[93] The immobilization step is also crucial, where the epitopes should not be altered.[94] Furthermore, the epitopes should be available for the binding reaction with the antibodies.[95] Unspecific binding and biomolecules denaturation, conformational changes are likely to happen in the case of a direct immobilization of biomolecules through covalent or electrostatic interactions on a surface, as well as a poor orientation. Unspecific binding on the surface can

be caused by polar and non-polar residues, for example, or ionic and hydrophobic interactions.[96] In case of possible unspecific bindings, blocking steps in the assay are often used such as in the gold standard ELISA.[97] In this assay, protein stability, high background, cross-reactivity, low loading capacity and sensitivity still need to be improved.[98]

2.7.2 Biosensing Principles

A biosensor is an analytical device composed of a biological component (recognition element) and a physico-chemical detector (transducer). The biological element can be tissues, antibodies, enzymes, cell receptors, nucleic acids, a biological natural element, or a biomimetic element that is going to interact with the element to be detected (called analyte), described in Figure 6. The transducer is divided into subclasses depending on the method of detection; it can be optical, electrochemical, amperimetrical, electro-chemiluminescent, piezoelectrical, and so on. This will transform the biological signal into another signal that can be detected and quantified via the transducing element. This part will also determine the sensitivity of the biosensing method. A subclass of biosensors is the immunosensors. They utilize the very specific interaction between Abs and antigens, and in combination with a tracer (fluorescence molecule, enzyme or radioisotopes) can generate a readable signal.[99]

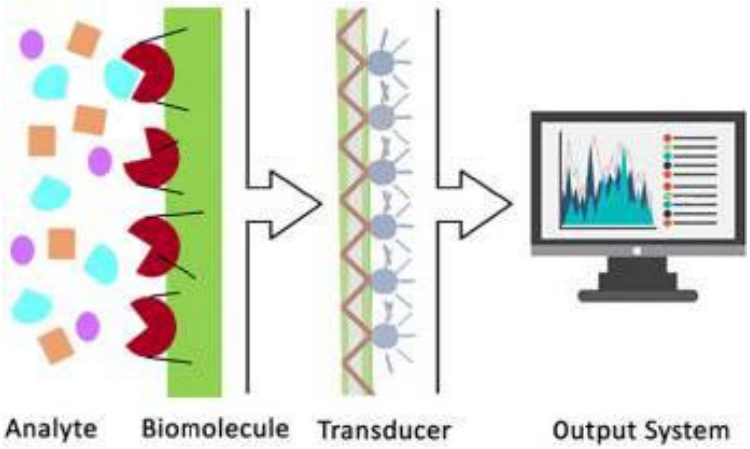

Figure 6. Representation of a biosensor. A basic biosensor is composed of a transducer with an output system, a biomolecule of recognition and the aim is to sense and quantify the analyte. Reproduced with permission from ref. [100]. Copyright © 2019, Emerald Publishing.

There are three generations of biosensors. First generation of biosensors detects the increase of products or the decrease of reactants using natural mediators for electron transfer.

One main example is by Clark et al. (1962) measuring blood oxygen content by mixing the blood with an hemolyzing solution (acid) and the content of released carbon dioxide and oxygen are measured. The carbon dioxide content was measured by diffusion of the acidic solution through a membrane into an alkaline solution. Furthermore, the glucose content is then monitored by the drop in pH of the solution. By using a hydrophobic membrane, the amount of glucose was determined by the reduction of dissolved oxygen concentration.[101]

Second-generation biosensors use redox mediators for a better sensitivity compared to the first generation. Some examples of mediators are organic dyes, ferrocenes (effective), quinones (biocompatible, simple synthesis, functionalization), and ferro-/ferricyanides (cathodic electron acceptor, rapid reaction, reversible).[102]

In third-generation biosensors, redox enzymes are fixed on the electrode surface which allows a more rapid electron transfer between the enzyme and the transducer.[103]

Biosensor materials are growing rapidly due to their potential in early-stage detection of disease and monitoring. They are used in many applications such as agriculture, environment, food quality, and security among others. For such devices to be effective, some criteria are needed, such as selectivity, specificity, high sensitivity, short time of detection, low limit of detection (LOD), and good precision. Selectivity is the ability of the device to detect the analyte in the presence of interferences (other unspecific biomolecules). The detection process should be precise with a high sensitivity (slope of the calibration curve). The LOD is the minimum amount of analyte that gives an identifiable output signal different from the blank. The LOD is dependent on the affinity of the analyte to the molecule of recognition, which is characterized by the dissociation constant K_d, where a low LOD requires a low K_d, meaning that the affinity of the biomolecules is high. Response time should be as quick as possible, which is defined by the time needed for the system to come into equilibrium (Figure 7). Some other parameters are also desired in biosensing such as a long shelf lifetime (time that the biosensor remains usable), good reproducibility and stability, low price, small size (miniature), good signal-to-noise ratio, user-friendly, and reusable. [100, 104]

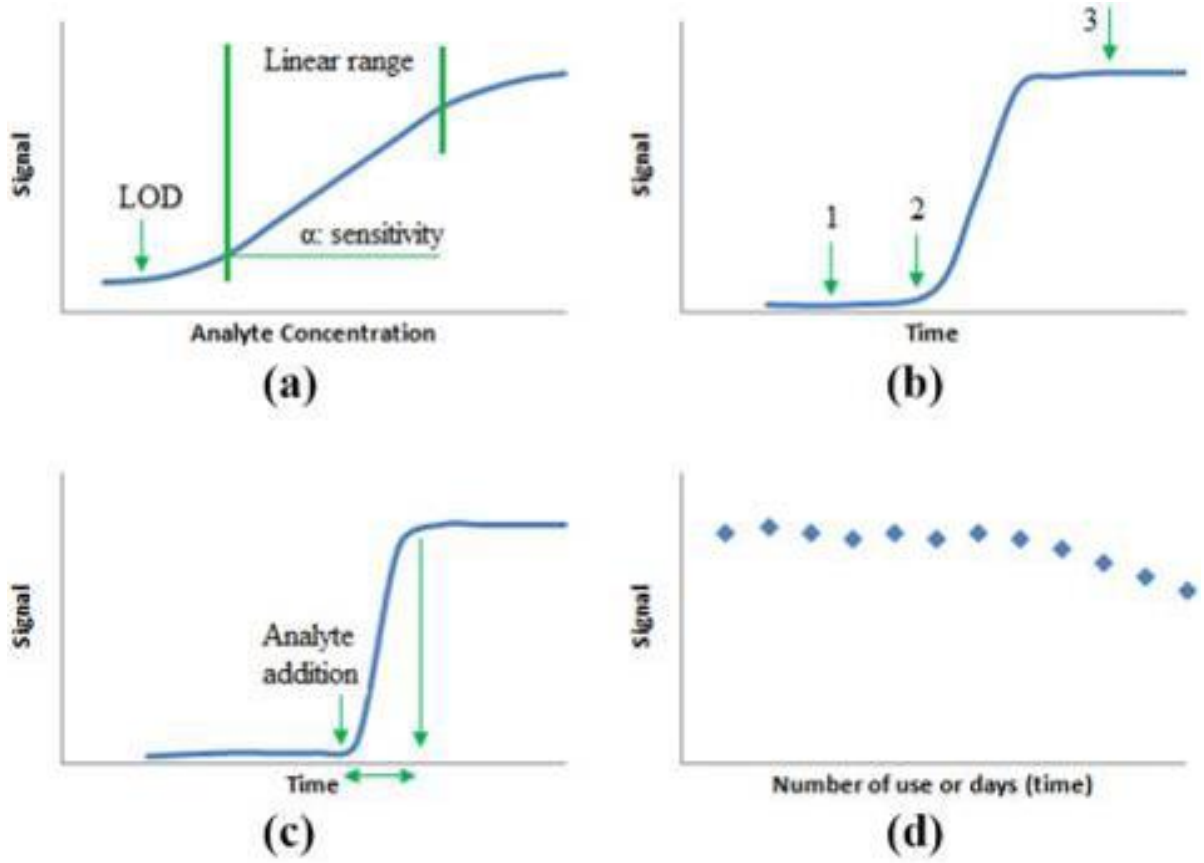

Figure 7. Summary of the main characteristics of a biosensor. (a) LOD, linear range, and sensitivity, (b) selectivity with a system selective to analyte 2, as an example, (c) response time, and (d) reusability and shelf life. Reproduced with permission from ref. [100]. Copyright © 2019, Emerald Publishing.

2.7.3 Fluorescence Biosensors

Fluorescence biosensors utilize fluorescence as transducing technique and measure the concentration of an analyte tagged with a fluorophore.[105],[106] Fluorescence is the property that fluorophores or fluorescent dyes (heterocycles, polyaromatic hydrocarbures) possess. Fluorescence results from a three-step process: excitation, excited-state lifetime, and fluorescence emission. The phenomenon is described in the Jablonski diagram (Figure 8). Basically, fluorophores can emit a photon shortly after absorbing one with a higher wavelength. In the first step, a photon of an energy hv_{ex} is emitted by an external source (lamp, laser) and absorbed by the fluorophore, which creates an excited electronic singlet state (S_2). In the second step, the excited state remains for a small time (typically 1-10 nanoseconds) during which conformational changes occurs in the molecule. At this stage, S_2 is partially dissipated,

yielding a relaxed singlet excited state (S_1) from which fluorescence emission occurs ($S_1 \rightarrow S_0$). When excited by absorption, not all molecules return to the ground state S_0 (by fluorescence emission). Quenching, fluorescence resonance energy transfer (FRET), and intersystem crossing can also occur to depopulate S_1. The fluorescence quantum yield refers to the ratio of the number of photons emitted (last step) to the number of photons absorbed (first step). The difference in energy between S_1 and S_2 is the Stokes shift (hv_{ex} - hv_{em}). This parameter is essential for determining the sensitivity of the fluorescence technique since it allows one to detect emitted photons with a low background, determined from excitation photons. The difference of wavelength allows a high signal-to-noise ratio for fluorescence spectrometry, in contrast to absorption spectrophotometry which measures the transmitted light relative to the incident light levels at the same wavelength.[107]

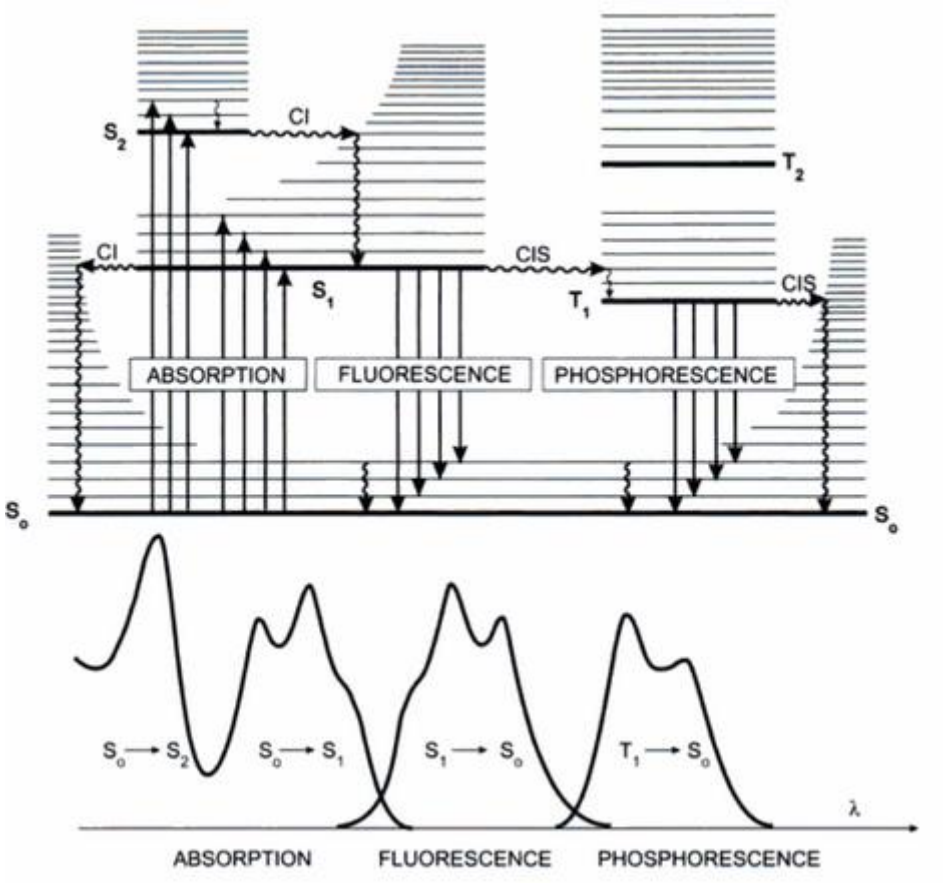

Figure 8. Jablonski diagram. Reproduced with permission from ref.[108] Copyright © 2013.

2.7.4 Immobilization of Biomolecules on Surfaces

The immobilization of biomolecules is critical in various applications to optimize the interaction with other biological species, the stability of the bio-species, and to ensure a proximity with the transducer to get an optimum performance of devices, systems, or apparatus.[109] Different techniques and strategies of immobilization of biomolecules are reported below (summarized in Figure 9 and 10).

Covalent Binding

This technique is the most used immobilization method. They enter in the irreversible reactions' category due to the robust and stable nature of covalent bonds. Covalent binding is achieved through functional groups present in the biomolecule of recognition, which do not play a role in their biological activity. Usually nucleophiles present on the amino-acid side chains are used such as amine, thiol, hydroxyl, or carboxylic groups.[110] In the case of DNAs, they require a linker functional group including succinimide-, aldehyde-, or maleimide-based groups.[111] Surfaces are usually activated and functionalized such as dextran, glass, or gel surfaces. Covalent immobilization prevents leakage of the biomolecules and a more stable system (Figure 9).[112]

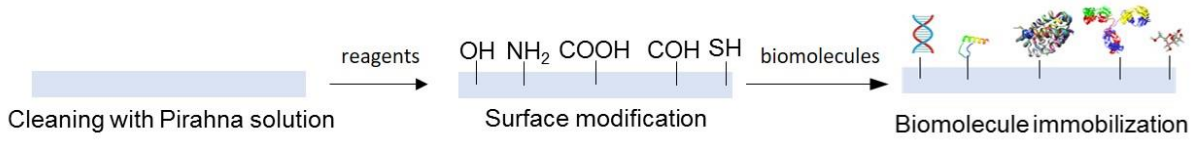

Figure 9. Schematic representation of different covalent strategies of biomolecule immobilization on a surface.

Schreiber Approach

The first microarrays have utilized the Schreiber approach, which consists in immobilizing proteins or peptides using nonspecific immobilization based on amine chemistry. The proteins are tethered to functionalized glass surface with aldehyde groups through their lysine residues and amines at the N-terminus.[113] To minimize unspecific protein interactions, bovine serum albumin (BSA) is used between the glass surface and the immobilized biomolecules.[114]

Membrane Protein Arrays

A membrane-like layer on glass slide is deposited using lipids anchored onto the glass surface previously modified with γ-aminopropylsilane. Proteins are spotted on the array on the membrane and anchored via noncovalent, hydrophobic interactions between lipids and the membrane proteins. Due to the random organization of the proteins, it is difficult to predict the sufficiency of exposure of the immobilized ligands, which often leads to impeding the binding event. This technique may also cause protein denaturation and loss of function and activity of the proteins.[115]

Oxime/Thiazolidine Formation

This technique results from optimizing the Schreiber method of immobilization, which lacked orientation thus effective interaction between the capture molecule and the analyte. The technique consists in a site-specific and covalent bindings to regiospecifically immobilize biomolecules on glass slides via glyoxyl derivatives that form oxime bonds or thiazolidine ring. Oxime bonds are however not very stable, and the use of this chemistry for large-scale production is difficult.[116]

Diels-Alder Reaction

In line with chemoselective immobilization, Diels Alder reaction is utilized to immobilize biomolecules on surfaces. For example, a cyclopentadiene-functionalized peptide was immobilized on a glass surface previously coated with a self-assembled monolayer (SAM) of alkanethiols with benzoquinone groups, which are the dienophiles. This reaction is rapid and effective and site-specific. SAMs are inert to proteins and no unspecific reaction occurs, removing the need of a blocking step.[117]

Staudinger Ligation

Another site-specific technique of immobilization of proteins is the Staudinger ligation. It consists in incorporating an azido group into a protein, which can react with a

phosphinothioester-functionalized surface to form an amide bond. The reaction is rapid, with a high yield, and occurs at room temperature.[118]

Crosslinking

Free reactive ends are used in the crosslinking technique. They form covalent bonds that anchor the biomolecules on the transducer surface. As examples, crosslinkers such as glutaraldehyde, glyoxal, and amine-based groups are used for crosslinking biomolecules to the surface. The issue in this method is to ensure that the conformation of the biomolecule or any function is not altered even slightly, since it may affect the binding event with the analyte. To prevent any loss of function, polymer networks can be used, especially for species like cells, proteins, and enzymes.[110, 119]

Entrapment

The method consists in entrapping a biomolecule in a polymeric network prepared in a solution containing the capture biomolecule. The network is in principle permeable to the analyte while holding the capture biomolecule inside the polymeric matrix. No covalent binding is involved with the biomolecules. Typical polymers used are cellulose, polyacrylamide, chitosan, alginates, and many others. Entrapment is the easiest method of biomolecule immobilization. This configuration also enhances the biomolecule stability and allows one to tune the properties of the network optimal for the biomolecules' environment. The disadvantage is the possibility of leakage and a limited mass transfer of the analyte into the network.[120]

Adsorption

This is the easiest method, which consists of adsorbing the capture ligand to the surface using hydrogen bonds, Van der Waals forces, salt linkage, or through electron transition complexes. This method is common for cell immobilization, and examples of surfaces are cellulose, glass, hydroxyapatite or collagen, polyethylenimine, polyaniline, polystyrene or polypyrole, poly-L-lysine, and polyethylene glycol. However, the disadvantages of this method are numerous: the orientation of the biomolecule is random, the reproducibility is limited, and the system is sensitive to physical stimuli (pH, ionic strength).[121]

Affinity Binding

Carbohydrates Immobilization

Carbohydrate and nitrocellulose have a strong noncovalent interaction. Glycans, including polysaccharides, glycoaminoglycans, glycoconjugates, and glycoproteins, have been used and attached to a nitrocellulose-coated glass surface. The system can be used to detect protein-carbohydrate interactions. This technique has been used as an example in the detection of pathogenic strains of *E. coli* in human serum.[122]

Protein - Protein, Avidin - Biotin Immobilization

Affinity binding technique involves noncovalent bonds depending on affinity bonds between the substrate and the analyte. The affinity between lectin and sugar, for example, or antibody-antigen can be used for immobilization. A strong binding affinity is streptavidin-biotin with a $K_d = 10^{-15}$ M.[123]. Avidin is a very stable protein and avidin molecules bind rapidly and almost irreversibly to biotin. This also prevents nonspecific interaction with other proteins thus eliminating any blocking step in the procedure, which also minimizes the background signal.[124]

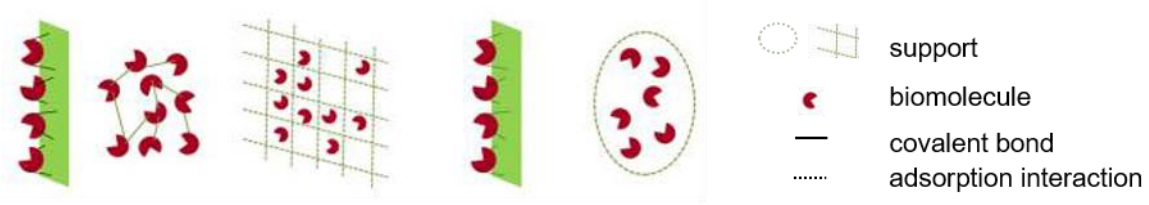

Figure 10. Schematic representation of different strategies (covalent binding, entrapment, crosslinking, affinity binding, and adsorption) of biomolecule immobilization. Modified reprint with permission from ref. [100] Copyright © 2019, Emerald Publishing.

2.8 Bio-responsive hydrogels

2.8.1 Definition and concepts

Bio-responsive hydrogels are the type of biomaterials that change their properties in the presence of a specific biological target.[125] The concept is to trigger a molecular interaction

that will therefore translate into a macroscopic response, for instance, a swelling/shrinking, an optical change, and a sol-gel transition.[126] Such materials are interesting for many applications needing a direct read-out or a capture/release of a target species (drug delivery, biosensing, cellular studies, biological sponges, and tissue regeneration).[127] They present many advantages such as providing a wet hydrophilic environment, optimal for biological interactions and stability. Also, there are few chances of nonspecific interactions when using antifouling polymers. Moreover, a wide range of chemistry is usable to build a matrix that can incorporate biomolecules. In addition, hydrogels are easily tunable in terms of mechanical properties while having the ability to change properties under stimuli such as pH, temperature, ionic strength, solvent polarity, light, magnetic/electric field, molecules, and biomolecules.[5c, 128]

Bio-responsive hydrogels are obtained by various methods and one of them is molecular-imprinting polymers.[129]

2.8.2 Molecular Imprinting Technique (MIT)

Molecular imprinting is a method aiming to leave an imprint into a polymer network with a shape memory of the template molecule. This will allow the formation of specific recognition sites within the solid.[130] This was inspired by the specific recognition of antibodies to antigens where antibodies adopt a three-dimensional complementary structure by contact with the specific antigen. This method is used in many applications such as biosensing, separation materials, assay systems, and catalytic applications.[131] They are also used in an industry scale production due to their low cost and stability.

Two pathways can be used to imprint molecules, biomolecules, bio-species, and others (Figure 11). Both approaches involve the choice of the monomer that can create a covalent or non-covalent bond with the necessary moiety to interact with the desired template molecule. These monomers are polymerizable and crosslinked to form a polymer network where the template is entrapped. After the removal of the template, specific recognition sites remain in the porous network where the pores correspond to the shape of the printed entity. This gives in the end an artificial recognition matrix.[132]

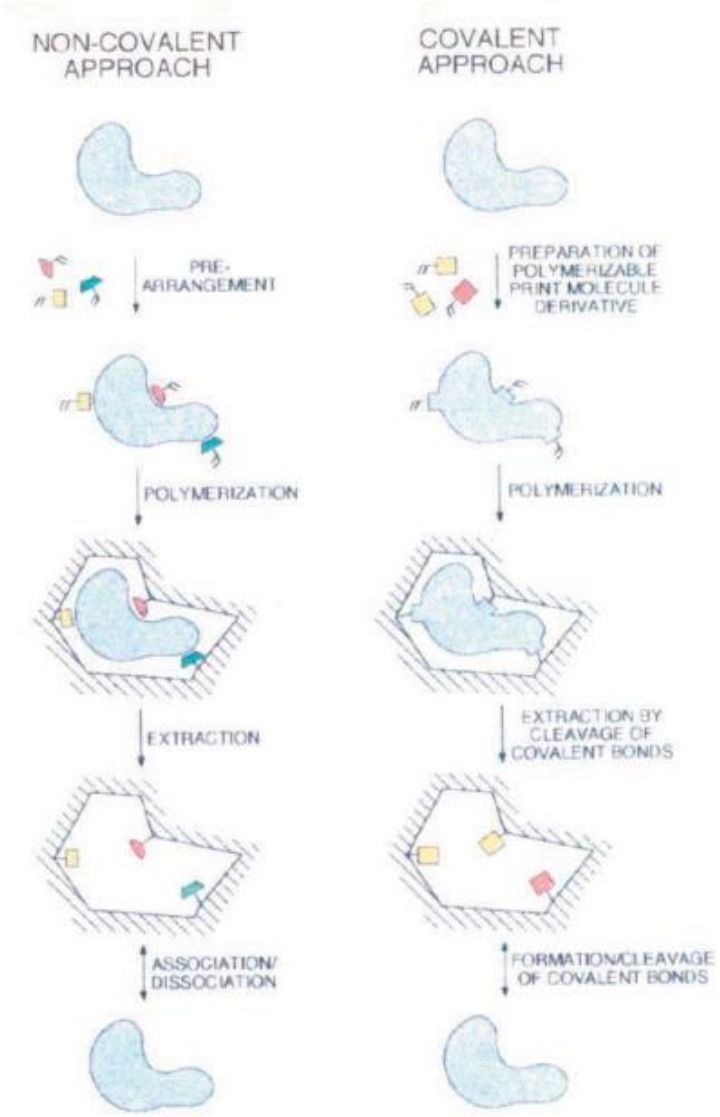

Figure 11. Schematic representation of the concept of molecular imprinting by two ways (covalent and non-covalent approaches). Reprint with permission from ref. [133]. Copyright © 1996, Nature Publishing Group.

Non-covalent imprinting

Non-covalent imprinting involves a complex formation with non-covalent binding between the template molecule and the surrounding polymer. Because biological recognitions are mainly based on non-covalent interactions, many systems of imprint used this method of imprint. Common interaction types are ionic interactions, π-π interactions, hydrogen bonds, or hydrophobic interactions.[133]

Covalent imprinting

Covalent imprinting involves a complex formation with covalent binding between the template molecule and the surrounding polymer. These covalent bonds must be cleavable. Therefore, functional groups such as esters of carboxylic or boronic acids are used; other examples are imines or ketals. The cleavage is usually performed by acid hydrolysis.[134]

Since the synthetic pathways to obtain a reversible covalent binding is very limited, non-covalent imprint is more often used for its versatility. Although both covalent and non-covalent approach can be used for imprinting a more complex molecule or molecules difficult to imprint.[133-134]

2.9 Human Mesenchymal Stem Cells (hMSC)

2.9.1 Definition and General Information

Mesenchymal stem cells (MSCs) are pluripotent stromal cells with an important expansion ability that have the particularity to be able to differentiate into varieties of cell types such as osteoblasts, chondrocytes, myocytes, and adipocytes. They are present in multiple tissues, including umbilical cord, menstrual blood, bone marrow, and fat tissues. Recently, they are seen in several applications, such as cell-based therapy, regenerative medicine or tissue engineering. In therapy, only certain hMSCs are used.[135] The Mesenchymal and Tissue Stem Cell Committee of the International Society for Cellular Therapy asserts that the minimal criteria to define a cell as hMSC are the following: "(i) hMSC must be plastic-adherent when maintained in standard culture conditions, (ii) they must express CD105, CD73 and CD90, and lack expression of CD45, CD34, CD14, or CD11b, CD79alpha, or CD19 and HLA-DR surface molecules, (iii) they must differentiate to osteoblasts, adipocytes, and chondroblasts *in vitro*." Additionally, for certain clinical applications, CD73, CD90, and CD105-positive hMSCs are used. The important challenge in these fields is then to provide stem cells with intact stemness. In *in vitro* expansion, the substrate will play a key role.[135-136]

2.9.2 Mechanical Response of hMSCs to the Substrate

The hMSC-matrix interface is dynamic and properties of the material of the cell scaffold such as stiffness, topography, molecular flexibility, and binding affinity; chemical functionalities influence cells behavior (Figure 13). These phenomena are also seen in their natural cell niche where the cell-environment is not static. Different organs and tissues have different stiffness, topographies, and chemical functionalities among other properties.[137]

Stiffness has an impact on the specific lineage differentiation (Figure 12). As a result, hydrogels have emerged as optimal materials for tuning the stiffness since their mechanical properties can be simply influenced by a change in crosslinking density, linker properties, or porosity. They can range from ultrasoft (E < 1 kPa, viscous fluid-like materials) to ultrahard (< 500 kPa, silicon rubber), while biological tissues can range from 0.1 kPa (neural cells) to 40 kPa (non-mineralized bone tissue). Common polymer used for fabricating hydrogels as substrates are polyacrylamide-coupled glucamine to avoid unspecific protein interactions, also polyethylene glycol, hyaluronic acid (4 - 100 kPa), and alginate (1 - 160 kPa). More and more research is now also directed towards more complex viscoelastic behavior with a dynamic change in stiffness and frequency-dependent stress responses.[138]

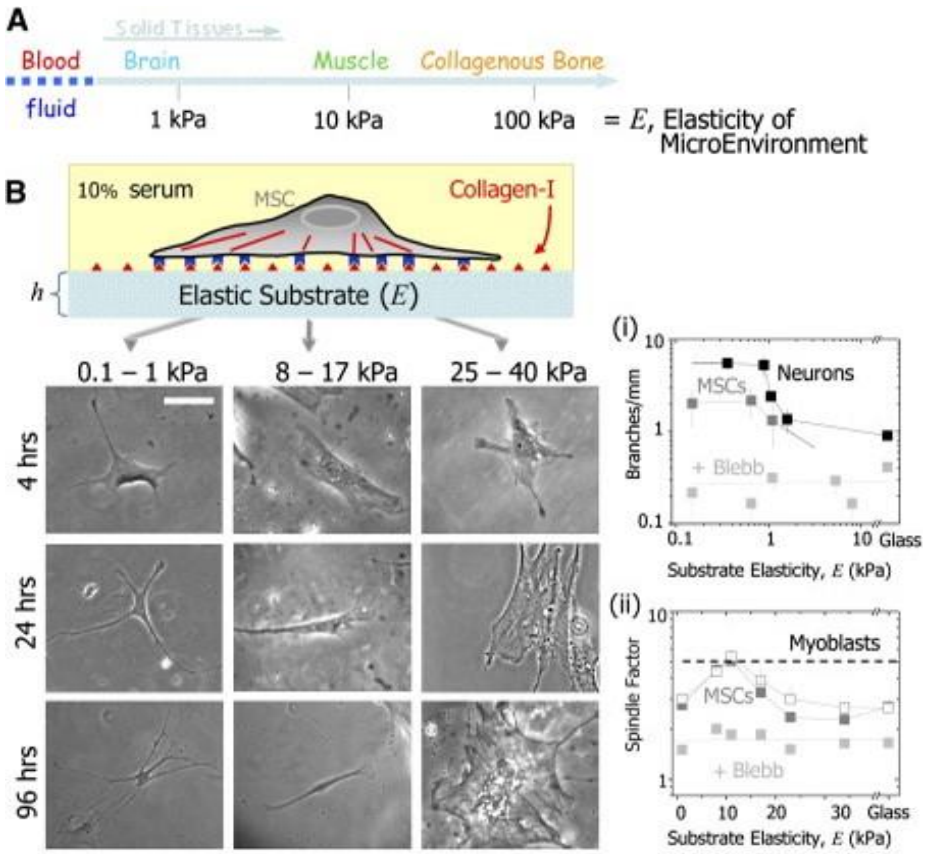

Figure 12. Biological tissue elasticity and differentiation of hMSCs. (A) Range of stiffnesses of different biological tissues. (B) Elasticity is controlled by crosslinking and cell adhesion by

attachment of collagen-I with control of the thickness. Scale: 20 nm. Morphological changes of the hMSCs are depicted as a function of different stiffness of the substrates. Reproduced with permission from ref. [138b]. Copyright © 2006, Elsevier.

During the first days of culture, reprogramming the lineage specification of hMSCs is possible by adding induction factors in the medium. However, recent studies have shown that the cells after several weeks will commit to the specification induced by the matrix elasticity.[138d] For example, soft matrices, a mimic of brain tissues, would lead to neurogenic differentiation, and a stiffer matrix (muscle mimicking) will lead to myogenic differentiation.[138b, 138c] These results enhance the impact of substrate stiffness in the stem cells differentiation.

Topographies can be tuned by nanolithography, molding, and electrospinning. Nanolithography can be used to control the spatial organizational symmetry of nanometer-scale patterns on a material's surface. Channels and pillars can be varied to mimic the natural arrangement of natural ECM.[139] As an example, nanopillars can be arranged in hexagonal or honeycomb structures, or in microgrooves, nanodots, and nanopits. This has, for example, supported the renewal of embryonic stem cells, hMSCs, and other cells. Electrospinning technique forms nanofibrous structures from polymers, where the nanofibers and nanochannels can be tuned to mimic the ECM naturally present in the body with fiber sizes of 5 to 200 nm and pore sizes from 3 to 80 nm.[140] Techniques using molding strategies can be utilized, such as on poly(hydroxyethyl methacrylate) (PHEMA) hydrogel networks utilizing PDMS stamps.[139-141]

Various strategies can be used to link cell-adhesion protein or peptides and growth factors and glycoproteins to the hydrogels. For instance, methacrylate functional groups are incorporated into PEG hydrogels by photopolymerization designed to covalently attach peptides. In these studies, the cell fate is influenced by these biomolecules attributing the effect to the adsorption or sequestering of these molecules into the matrix.[142] Other than only biomolecules, chemical compounds can also influence the cell differentiation, for example, the release of calcium and phosphate ions influenced differentiation to osteoblasts through mechanism that involved c-Fos and adenosine signaling.[143] Other examples are fluoride, strontium, and magnesium release, which have also changed cell phenotypes.[142-144]

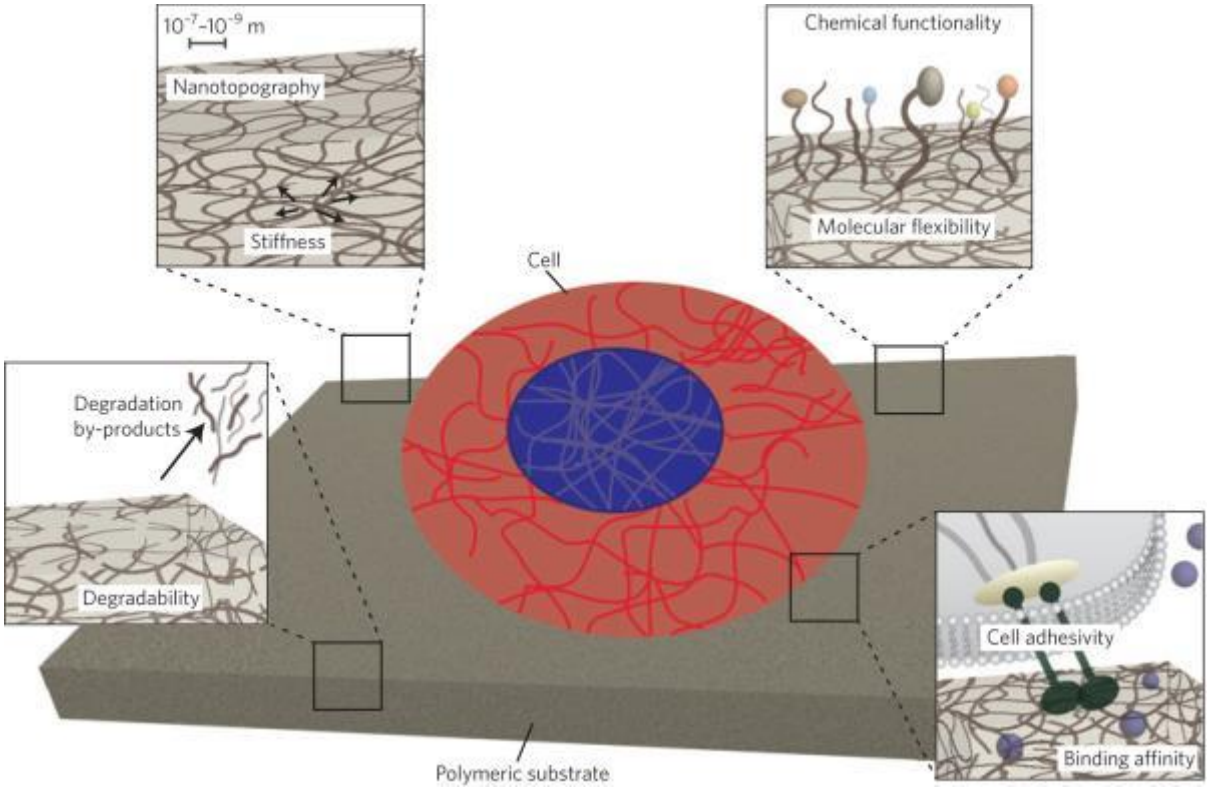

Figure 13. Summary of the parameters that have an influence in cell phenotypes such as topography, chemical functionality, degradation of byproducts, in the case of degradable hydrogels, and cell adhesivity on polymeric substrates. Reproduced with permission from ref. [143]. Copyright © 2014, Nature Publishing Group.

We have learned that the interface of the cell and substrate is dynamic more than static and that the cell interacts with the surface, which regulates the cells' functions both in the short and long term. Studies have shown that the cell differentiation was influenced by the substrate stiffness independently of the porosity and protein tethering. Stiffness is thus one of the main mediators of cell functions.[145] The interaction of the cell with the substrate goes beyond biological exchanges but the cell matrix is also a physical interaction, which leads to matrix deformations (Figure 14). Indeed, cells sense the substrates' elasticity by local contractions.[146] Myosin contractions can induce cells to pull substrates at a rate of 20 to 120 $nm.s^{-1}$. Therefore, deformations of the substrates become visible. These deformations are inversely proportional to stiffness.[145-147]

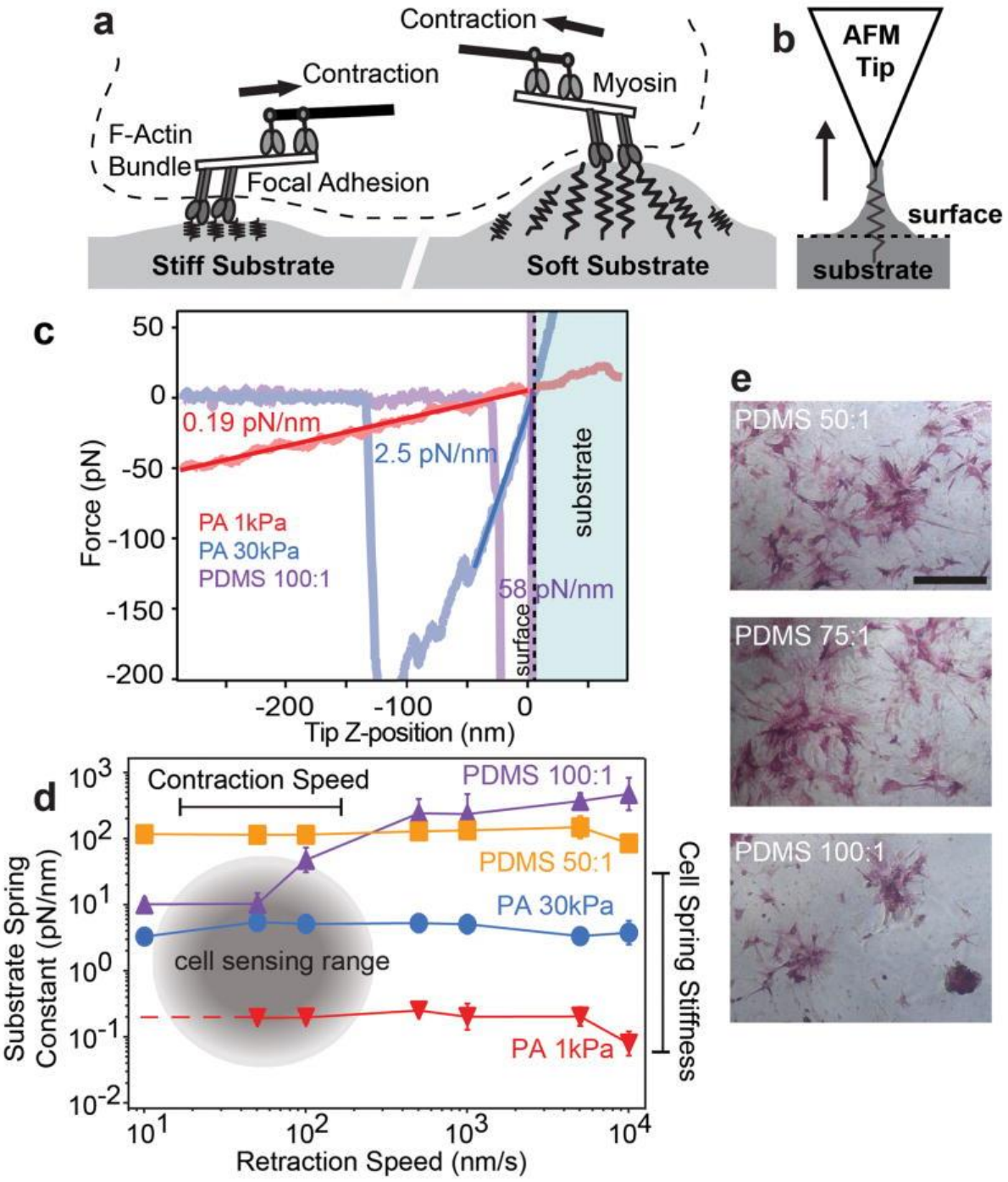

Figure 14. Studies of cell contraction against hard and soft substrates by atomic force microscopy (AFM). (a) Cells dynamically interact at the interface to deform the substrate by pulling through myosin contractions. Soft substrates are more deformed than stiffer ones. (b) Scheme of the interaction of AFM tip with the substrate. (c) Representative retraction curves of different hydrogel stiffness. (d) Substrate spring constant as a function of AFM tip retraction speed. (e) APL staining of cells on PDMS substrates after 7 days of culture in medium where the cells differentiated into osteoblasts. Scale: 500 nm. Reproduced with permission from ref. [146] Copyright © 2014, Nature Publishing Group.

2.10 Tissue Engineering

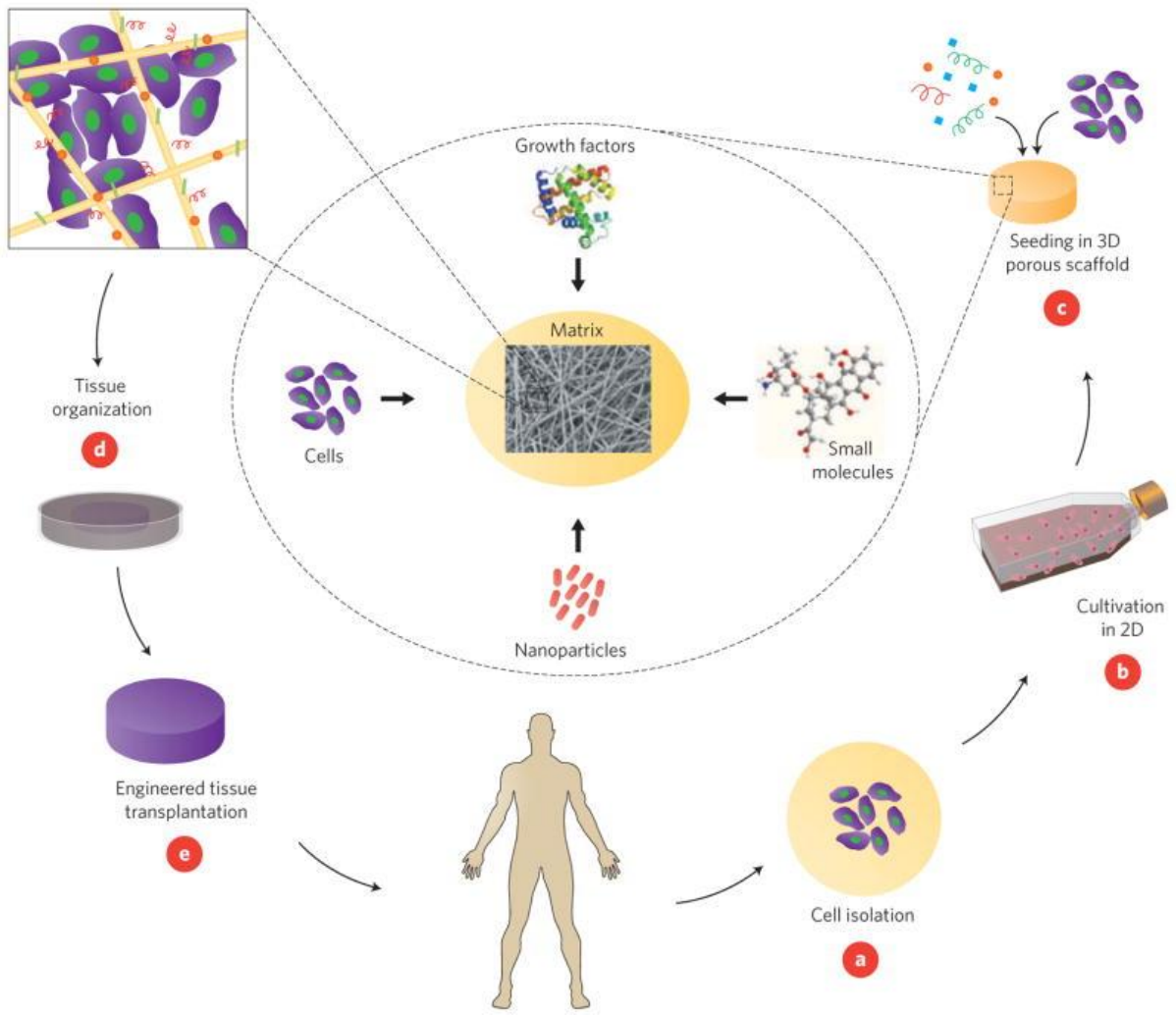

Figure 15. An example of a tissue engineering strategy summarizing four important factors that need to be considered in tissue engineering: the cells, the scaffold (environment that supports the cells), biomolecules, such as growth factors molecules, physical and mechanical forces to influence the cell fate. Reproduced with permission from ref. [148]. Copyright © 2010, Nature Publishing Group.

Tissue engineering aims to create a functional tissue from cells in a laboratory to replace or repair failing tissues or organs due to disease, genetic abnormalities, trauma, or injury. Indeed, tissue injury or organ failure is considered a major challenge in healthcare. The field has emerged as a result of a limitation of transplants from donors. Before the 1950s, no suitable

remedies existed for patients with organ dysfunctionalities. Only with the pioneering work of Murray in 1964, with the first successful kidney transplant, the field has started to evolve. Yet, the donor was a twin brother of the patient so the risk for an adverse immune response was eliminated because the donor and recipient were genetically identical. Five years later, Murray performed a transplant from a genetically non-identical donor on a patient, a procedure, which has then served to save several lives. However, the increasing number of patients needing organs transplants and the shortage in organ donors limits the method, which requires the development of new methods to repair tissue and organ defects.[8b, 149]

Four important factors need to be considered in the tissue engineering: (i) the cells, (ii) the scaffold (environment that supports the cells), (iii) biomolecules such as growth factors, (iv) physical and mechanical forces to influence the cell fate.[148] The cells can be harvested from the target organ, from stem cells, or directly taken from the patient to limit rejection issues. The scaffold can be natural (collagen, decellularized matrix, etc.) or synthetic (mimicking the cell environment, for example, extracellular matrices (ECM)) or derived from donor tissues and can be degradable or not depending on the application (Figure 15). Synthetic scaffolds must be fabricated with specific features such as permeability, optimal spatial distribution, porous materials with optimal pore size, because the bulk and surface characteristics of the scaffold might affect the cellular behavior during the cellular growth. One important challenge in tissue engineering is the need of a large cell quantity and to engineer thick tissues, ultimately organs, vascularization is key. Furthermore, individual cells' performance and their interaction with the ECM influence in the end the organ function. That is why providing biomaterials to allow different cells to act in the optimal way is a major challenge in the field.[8b, 150]

Another aspect to consider in the development of materials for tissue engineering is the material's properties using nano- and micro-technologies. Micro- and nano-patterning can control cellular behavior as well as the cell environment at different levels, for example adhesion, locomotion, proliferation, and differentiation. Cell shape, cell interaction with the matrix, and cell-cell interactions have been controlled in microarrays as an example. Another example is the culture of neural stem cells in a specifically spatially distributed proteins in a matrix, which showed an alignment of neurons.[151]

Bioprinting

3D printing is a technique that consists in precisely depositing different materials on various substrates. The method has been extensively used in tissue engineering to print cells, scaffolds, or cell-laden hydrogels. For example, polyester urethane urea was used as a cardiac patch that was patterned with hMSCs and endothelial cells. The patches were implanted into rats with myocardial infarction and showed after insertion of the patch, an increased vessel formation and an enhanced heart function. The same method was used for the fabrication of heart valves by using encapsulated valvular interstitial cells into methacrylated hyaluronic acid or gelatin hybrid hydrogels.[152]

2.11 Soft Tissue Engineering

Soft tissue engineering focuses on providing substitute tissues to restore damaged or deficient tissues including fat, muscles, tendons, vessels, nerves, skin, and ligaments. This area is challenging since it aims to restore defects with a high volume to surface area. As an example, techniques for damaged tissue beneath the skin are divided in two main categories. The first category aims to use synthetic substitutes from the formation of new adipose tissue from precursor stem cells (called *de novo* adipogenesis). In this way, the differentiation is guided towards adipogenesis via different strategies. The second approach is an autologous fat transfer. This second method is relatively limited since graft retention rates can fall until 90% over time due to necrosis, cysts, and granulomas. The understanding of *de novo* adipose tissue formation will allow the design of implantable matrices and master the adipogenesis pathway.[153]

De Novo Adipogenesis

Differentiation into adipocytes is dependent on glycerol-3-phosphate dehydrogenase (GPDH). The action of this enzyme allows the accumulation of intracellular lipid droplets. Other markers for adipogenesis are perosixome prolerator-activated receptor gamma, lipoprotein lipase (LPL) and fatty acid binding protein (FABP)-4. Adipocytes absorb triglycerides from the microenvironment using LPL uptake for example. *De novo* adipogenesis approach requires an *in vitro* expansion and isolation, which raises feasibility hurdles.[154]

Autologous Fat Transfer

Although the existing drawbacks of autologous fat transfer, namely, graft rejection, efforts are directed towards preventing these rejections. Recent research has shown that the incorporation of progenitor cells such as ASCs might improve the approach. The technique consists of injecting ASCs into the fat (cell-assisted lipotransfer (CAL)). Clinical results have suggested that the presence of ASCs have enhanced the grafted tissue viability and 5.10^4 supplemental ASCs per milliliter of transferred fat would be necessary to get best results.[155]

2.12 hMSC Culture Scaffolds

The complex organization of tissues in the body allows cell-cell and cell-environment interactions. Synthetic polymers are the most used as scaffolding materials for soft tissue engineering.[156] Their advantage is the possibility to tune their physical properties, and the existing large number of FDA-approved polymers. Synthetic polymers have been utilized to mimic the architecture of natural collagen, PLGA, PEG-based polymers, and PVA, for example, which has been shown to enhance cell adhesion and to allow differentiation. Synthetic scaffolds should be developed to mimick the native structure of the tissue and should be engineered for cells to be able to adhere, proliferate, spread, differentiate, and act like they would *in vivo*. The choice of the scaffold is crucial since it strongly influences the cell fate.[138b] Therefore, materials selection depends on mechanical properties that favor highly porous materials with interconnected pores to allow free diffusion of cell nutrients and oxygen, which allows the cells to migrate. Topography can also influence the cell differentiation and the materials' surface plays a key role for cell interactions. In addition, to tailor the cell response to the material, functionalization of the surface with for example proteins or peptides, typically RGD, as integrin-binding domains.[157] Surface modification should be done after fabricating the scaffold to not alter the mechanical properties or structure. Finally, top-down and bottom-up strategies are used to build a scaffold where a top-down method designs a scaffold that mimic tissue (structure, composition and mechanical properties) and a bottom-up approach consists in mimicking and replicates the main unit of a tissue to get the proper scaffold.[157-158]

3 Scientific Goals

The aim of this PhD thesis was to explore multi-disciplinary domains to provide solutions for current challenges in the biomaterial field, namely, detection of antibodies, and thereby developing a material for an ultimate use in biosensing devices. In a second project, the aim was to contribute to the development of new polymeric scaffold for tissue engineering, and cell-based therapy. The goal is therefore proposing a substrate that mimics the natural environment of sensitive human stem cells to keep their "stemness" in a synthetic environment. In a third project, the goal was to develop a responsive hydrogel towards influenza virus giving a dual response (both color and shrinkage) to prove that such multivalent interactions are possible and specific. The first hurdle of these systems was to find an optimal hydrogel system to host the different biological species, which would lie in the fabrication of the matrix via different chemical routes, different molecules, and conditions. For each system, different parameters regarding their mechanical properties have been explored to get an optimal matrix. Therefore, to get a better understanding of the biomolecules and cells' behavior within these macromolecular systems, a deep characterization has been performed comparing different techniques to get as precise characterization as possible. Finally, the performance of the material towards each application has been assessed by different biological studies: biosensing, bio-responsiveness, and cell-related studies, respectively.

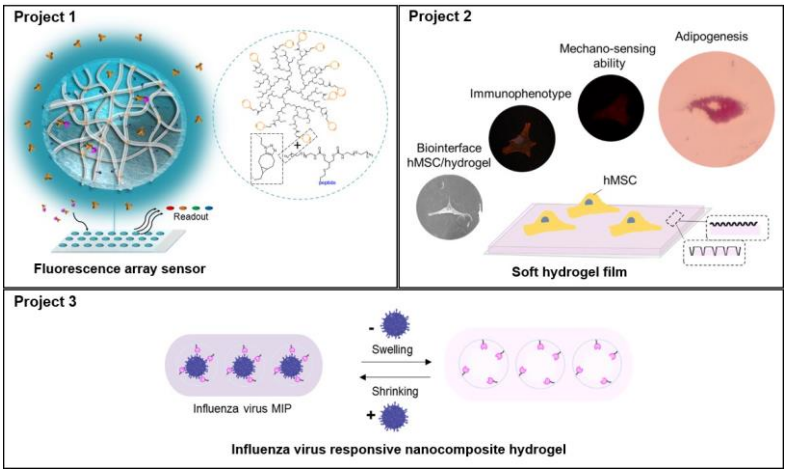

Figure 16. Summary of the projects within this PhD thesis. Three projects with two different applications are presented where hydrogels are used as main materials. The first project involves a hydrogel matrix biologically active with immobilized peptides within the matrix for the detection of specific antibodies. The second project consists of hydrogel nanocomposites as an optimal substrate for human mesenchymal stem cells' culture. The third project deals with hydrogel nanocomposite for the specific recognition of influenza virus.

4 Publications

In the following section, the published articles and submitted manuscripts are listed and the contributions of the author are specified

4.1 Highly Sensitive Detection of Antibodies in a Soft Bioactive Three-Dimensional Bioorthogonal Hydrogel

Rotsiniaina Randriantsilefisoa, José Luis Cuellar-Camacho, Mohammad Suman Chowdhury, Pradip Dey, Uwe Schedler, and Rainer Haag

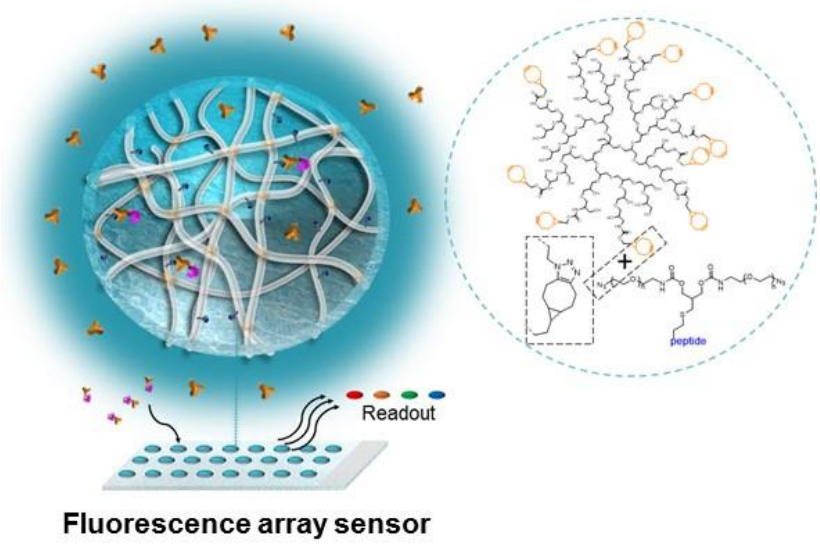

Author's contributions: In this publication, the author contributed to the concept, performed the synthesis, characterization (except AFM), did fluorescence measurements, evaluated data, as well wrote the manuscript. José Luis Cuellar-Camacho performed the AFM characterization, Mohammad Suman Chowdhury and Pradip Dey helped with the synthesis, Uwe Schedler and Rainer Haag designed the concept of the project and corrected the manuscript.

R. Randriantsilefisoa, J. L. Cuellar-Camacho, M. S. Chowdhury, P. Dey, U. Schedler, R. Haag, *Journal of Materials Chemistry B* **2019**, *7*, 3220-3231. https://doi.org/10.1039/C9TB00234K

4.2 Interaction of Human Mesenchymal Stem Cells with Soft Nanocomposite Hydrogels Based on Polyethylene Glycol and Dendritic Polyglycerol

Rotsiniaina Randriantsilefisoa, Yong Hou, Yuanwei Pan, José Luis Cuellar-Camacho, Michaël W. Kulka, Jianguang Zhang, and Rainer Haag

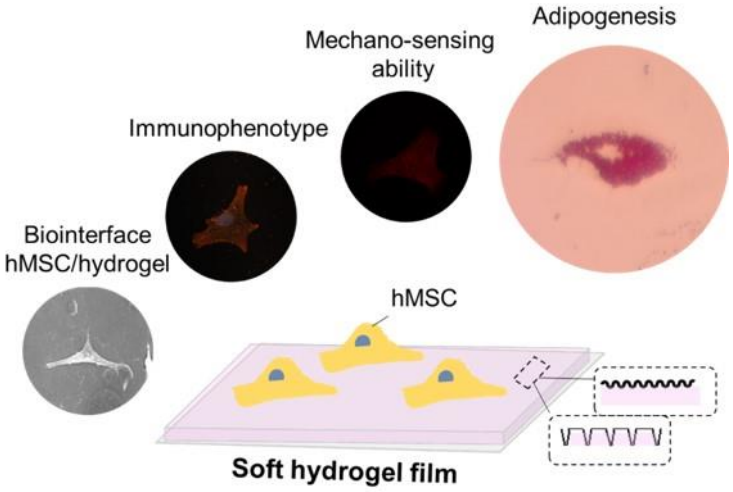

Author's contributions: In this publication the author designed the concept, performed the synthesis, characterization (except AFM and SEM), biological studies, evaluated data, as well wrote the manuscript. Yong Hou, Yuanwei Pan, and Jianguang Zhang helped with the biological aspects. José Luis Cuellar-Camacho performed the AFM characterization. Michaël W. Kulka performed the SEM characterization. Rainer Haag discussed the project and corrected the manuscript.

R. Randriantsilefisoa, Y. Hou, Y. Pan, J. L. C. Camacho, M. W. Kulka, J. Zhang, R. Haag, *Advanced Functional Materials* **2019**. https://doi.org/10.1002/adfm.201905200

4.3 Double Trouble for a Virus: Hydrogel Nanocomposite Catches Influenza Virus While Shrinking and Changing Color

Rotsiniaina Randriantsilefisoa, Chuanxiong Nie, Badri Parshad, Yuanwei Pan, Sumati Bhatia, and Rainer Haag

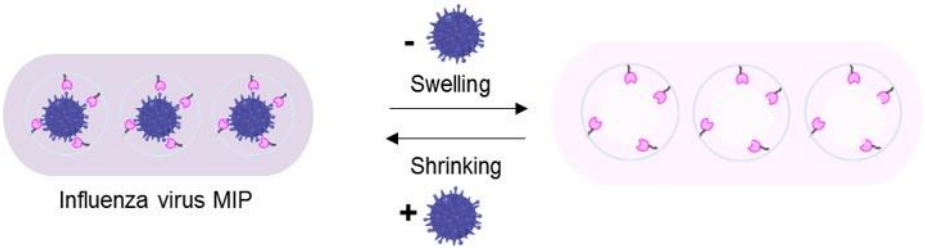

Author's contributions: In this publication, the author designed the concept, performed the synthesis, characterization, biological studies, the data evaluation, as well as wrote the manuscript. Chuanxiong Nie, Yuanwei Pan, Badri Parshad, and Sumati Bhatia provided the viruses, gold nanoparticles, sialic acid and corrected the manuscript. Rainer Haag discussed the project and corrected the manuscript.

R. Randriantsilefisoa, C. Nie, B. Parshad, Y. Pan, S. Bhatia, and R. Haag, *Chemical Communications* **2019**. Submitted.

ChemComm

COMMUNICATION

Double Trouble for Viruses: Hydrogel Nanocomposite Catches Influenza Virus While Shrinking and Changing Color

Received 00th January 20xx,
Accepted 00th January 20xx

DOI: 10.1039/x0xx00000x

www.rsc.org/

Rotsiniaina Randriantsilefisoa,[a,*] Chuanxiong Nie,[a] Badri Parshad,[a] Yuanwei Pan,[a] Sumati Bhatia,[a] and Rainer Haag[b,*]

We report a virus responsive hydrogel giving a dual response. The method utilizes the optical property of gold nanoparticles (AuNP) and the high swelling capacity of polyol-based hydrogels to form a nanocomposite of AuNP and polyols that produces both color changes and shrinkage in the presence of Influenza A virus particles.

Bio-responsive hydrogels are hydrophilic 3D networks that undergo a response triggered by the presence of one or several biological species.[1] Such materials have been used for detection, drug delivery, or tissue engineering applications.[2] More often, hydrogels responsive to small molecules have been utilized since engineering networks for macromolecules or multivalent molecules is challenging. First, molecular and architectural designs must be specific. Second, the complex interaction between the biological species and the matrix must be controlled. Finally the immobilization and the environment of the biomolecules must be such that denaturation does not occur.[3, 4] As examples of bio-responsive hydrogels, Miyata et al. have been working with ConA responsive networks.[5-8] Bai and Spivak have recently reported apple stem pitting virus-responsive superaptamer hydrogels.[9] They have shown the potential of bio-responsive hydrogels for virus detection. Some groups have also been working on dual-responsive hydrogels - giving a single response to two or more stimuli – such as Couturier et al. on photonic hydrogels for the detection of hydrophilic and hydrophobic bio-species.[10, 11]

Bioimprinting hydrogels with a biological entity template is becoming more and more popular in biorecognition, tissue engineering, or for cell culture platforms. Molecularly imprinted polymers (MIP) can offer a specific imprint of the bio-species of interest, which can consequently increase the sensitivity of the detection method, specificity to the cell interaction or give a conductive property.[12-17]

Gold nanoparticles (AuNP) are efficient for the immobilization of suitable molecules via physical adsorption or covalent conjugation. At the same time, their plasmon characteristics have made them a benchmark tool in domains of materials science involving, for example, optical detections.[15, 16] Having AuNP covalently entrapped in hydrogels offer a stable multifunctional material with plasmonic properties and, at the same time, leaching of the AuNP is avoided.[18]

Dendritic polyglycerol cyclooctyne (dPG-C) and polyethylene glycol diazide (PEG-DIA) are good polymer candidates for MIPs. It has been suggested in our previous work that a dPG-PEG-based network is an ideal anti-fouling environment for hosting delicate molecules such as proteins, peptides, enzymes, viruses, and antigens in general. They are naturally hydrophilic environments, robust, and constructed in a biorthogonal strategy, avoiding any unspecific interactions. Furthermore, they could swell up to 100 times their dry weight in the presence of an aqueous environment.[19]

Sialic acid (SA) has been reported to have a specific and high binding affinity with the hemagglutinin (HA) present on influenza A virus (IAV) in a multivalent manner. As a result, SA is an interesting candidate for building systems with specific interactions with IAV.[20, 21]

Therefore, herein we present a hydrogel using SA, PEG, dPG, and AuNP. In the present study, we aim to simply provide as a preliminary proof-of-concept for the ability of such hydrogels to display a reversible double response, both color change and shrinkage, in the presence of a saturating amount of specific IAV viruses.

[a, b] *Institut für Chemie und Biochemie, Freie Universität Berlin, Takustr. 3, 14195 Berlin, Germany.*
E-mail: haag@chemie.fu-berlin.de, rani2f@zedat.fu-berlin.de

† Electronic Supplementary Information (ESI) available: materials, experimental procedures, and additional results. See DOI: 10.1039/x0xx00000x

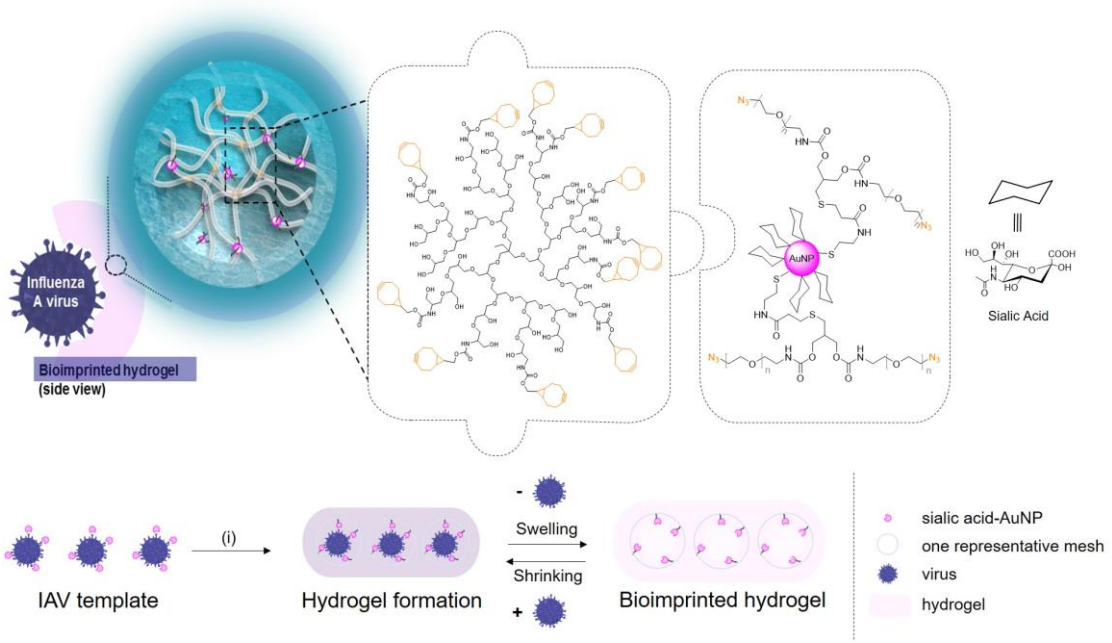

Figure 1. Representation of the hydrogel structure composed of clicked functional PEG and dPG. Formation of the bio-imprinted hydrogels with IAV: IAV is used as a template and mixed with a solution of sialic acid-functionalized AuNP. (i) The conjugated template is added in the hydrogel precursor mixture of dPG-C and PEG-DIA. The hydrogel is then formed by click chemistry. The virus is removed with 3.7 % HCl solution to produce an IAV-responsive imprinted hydrogel. An optical and mechanical response is produced upon IAV addition or removal.

Functionalized macromolecular precursors, dPG (MW. 10 kDa, 10 % cyclooctyne functionality) and diazide-PEG (PEG total MW. 6 kDa), quickly form a three-dimensional hydrogel structure via strain-promoted alkyne-azide cycloaddition (SPAAC) reaction. On the other hand, SA and PEG are conjugated to AuNP (20 nm) by means of electrostatic interactions and thiol-gold chemistry, respectively. The macro-porosity of the network is obtained by molecularly imprinting the hydrogel with IAV as templates. This forms in the end a hydrogel composite network imprinted with IAV for an enhanced specificity **(Fig. 1)**. The virus is removed by immersion of the hydrogel in a solution of 3.7 % HCl. The obtained hydrogels are then washed in distilled water until reaching equilibrium in color and size. During the process, a clear color change from purple (with viruses) to pink (without viruses) is noticed as well as a size change small (with virus) and bigger (without viruses). The virus release/uptake behavior of the hydrogel is evaluated by measurements of the hydrogel size and spectroscopic studies by UV-visible spectroscopy.

To first determine the optimal virus concentration needed as template, AuNPs decorated with SA (AuNP-SA) in solution are prepared and the interaction with viruses at different dosage is investigated (**Fig. 2**). AuNP-SA specifically recognizes IAV due to the known specific interaction between SA to the HA of IAV.[22] Viruses, as multivalent systems, can host multiple AuNP-SA via the multiple HAs on the virus envelope, which can lead to the aggregation of AuNPs in the solution. Due to the plasmonic properties of AuNPs, the IAV-AuNP binding can trigger the color change of the solution upon aggregation and dispersion. In the meantime, the aggregation produces a surface plasmon resonance (SPR)-induced absorbance shift in the absorption spectra, translated by a color from red to purple/blue detectable by eyes, along with an absorbance shift. When the particles are separated, the absorbance returns to its original value.[23] **Fig. 2** shows that the color shift in solution becomes more predominant as a function of the virus concentration. We observe in the photograph, a blue color for a concentration of virus of 4 * 10^8 pfu/mL, a purple color in the presence of a concentration of virus of 2 * 10^8 pfu/mL, and a light purple for a concentration of virus of 1 * 10^8 pfu/mL, a red color for the lowest concentrations and control (only PBS). This color change is quantified by the variance of the absorbance OD_{610}**.** For a virus concentration of 4 * 10^8 pfu/mL, the OD_{610} = 0.68, while at a virus concentration of 1 * 10^8 pfu/mL, the OD_{610} = 0.23.

The specificity in solution is explored by adding to it an unspecific virus to SA (VSV virus). The absence of response is noticeable with a very low OD_{610} of only around 0.15 whereas the specific IAV display an OD_{610} around 7 times higher.

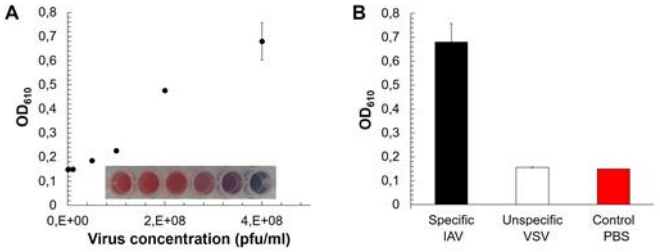

Figure 2. (**A**) Optical density at 610 nm as a function of different concentrations of IAV (4 * 10^8, 2 * 10^8, 1 * 10^8, 5 * 10^7, 1 * 10^7, 0 pfu/ml) and the corresponding photograph the solutions of SA-AuNP-IAV. (**B**) Optical density at 610 nm in response to unspecific VSV virus, specific IAV virus and only PBS (control).

After revealing the responsive behavior of AuNP-SA in presence with IAV, hydrogels are molded with AuNP-SA-IAV complex (virus concentration 5 * 10^7 pfu/mL, lowest concentration of color change noticeable by eye). The optical and mechanical changes in presence or absence of the specific or unspecific viruses are quantified by UV-vis spectroscopy and the percent of shrinkage by measuring the diameter of the hydrogels with and without virus.

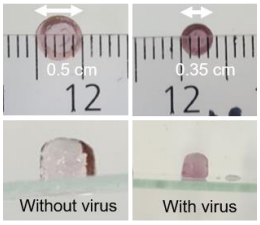

Figure 3. Photograph of the molecularly imprinted hydrogels with and without IAV (A/X31 (H3N2)), displaying a color change and shrinkage in the presence or absence of virus.

Fig. 3 shows that the hydrogels exposed to IAV viruses shrink and display a noticeable color change, compared to the ones without virus even though the color change is less predominant than the shrinkage.

The specificity of the system is studied by diffusion of unspecific and specific viruses in the hydrogels. **Fig. 4A** is the corresponding optical characterization of the bio-imprinted hydrogel with specific virus and with unspecific virus. Using specific IAV viruses, OD_{610} = 0.85 and OD_{610} = 0.6 without virus. In the presence of unspecific VSV viruses, is almost as low as without virus (OD_{610} = 0.5).

Afterwards, the reversibility of the binding and removal is studied by diffusion and removal of IAV viruses into the hydrogels. In **Fig. 4B**, different cycles of binding/removal of viruses with a saturating virus concentration of 1.2 * 10^9 pfu/ml are performed. The reversible increase/decrease in the OD_{610} demonstrates the reversible absorbance shift displayed by the hydrogels in the presence of IAV virus. At this saturation concentration, either most binding sites in the microporous hydrogel have been filled or no virus diffusion is no longer allowed due to hindrance. The number of binding sites is mostly linked with the template concentration used at first. Furthermore, the change of swelling state of the hydrogels in the presence of IAV viruses has been noticed.

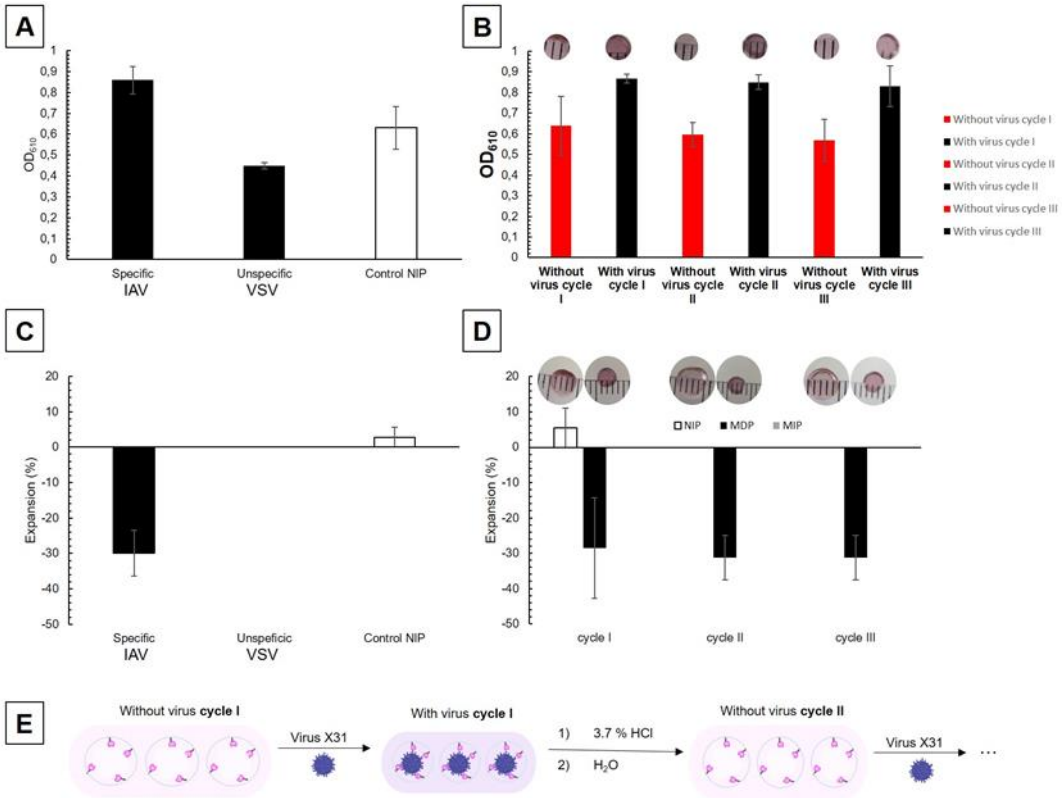

Figure 4. A. Optical density at 610 nm of the imprinted hydrogels in response to unspecific VSV virus and specific IAV virus, and non-imprinted hydrogels was used as controls. **B.** Optical density at 610 nm of the imprinted hydrogels ("MDP") in response to specific A/X31 (H3N2) virus (1.2 * 10^9 pfu/mL, 0.31 mg/mL HA) for three different binding/removal cycles. Control samples were non-imprinted hydrogels ("NIP"), and imprinted hydrogels without template removal ("MIP"). **C.** Percentage of MDPs' expansion (shrinkage) in response to unspecific VSV virus and specific A/X31 (H3N2). NIP and MDP were used as controls. **D.** Percentage of MDPs expansion (shrinkage) in response to specific A/X31 (H3N2) virus (1.2 * 10^9 pfu/mL, 0.31 mg/mL HA) for three different binding/removal cycles. Control samples were NIP and MIP. **E.** Schematic representation depicting the process used for three cycles of virus binding/removal.

In **Fig. 4C**, when the hydrogels are exposed to a saturating concentration of IAV, a shrinkage of the hydrogels appears. This phenomenon is due to supplemental crosslinking points provided by the multivalent binding between HA of the IAV and SA. The consequence being a higher crosslinking density in the network, translated by a shrinkage of the hydrogel.[5] Control experiments IAV diffusion into hydrogels without imprinting "NIP") are performed to verify that the given response is specifically due to IAV, also that the virus imprints are important to create responsive hydrogels with specific sites (**Fig. S8**).

To further characterize the mechanical reversibility, the hydrogels are subjected to multiple cycles of binding and removal of viruses. We hypothesize that the hydrogels would give a reversible swelling/shrinking depending on the presence or absence of IAV virus. **Fig. 4D** is a characterization of imprinted hydrogels for different cycles of binding and removal of viruses. We see that each uptake of virus can lead to a shrinkage (~ 30 %) with a relative recovery of the values for each cycle of virus binding or removal.

In conclusion, a proof-of-concept has been presented by developing a hybrid hydrogel which has the ability to show dual response to one biological stimulus (IAV). The combination of different materials has allowed the performance of the hydrogels, where inorganic components such as AuNP and organic hydrophilic compounds such as polyols have allowed both a color property and a high swelling and shrinkage capacity of the network. This also represents a sensitive environment to bio-species preventing their denaturation. The saccharides SA confer the specificity of the hydrogels towards IAV. Finally, the bioimprinting process gives an imprint specific to IAV and simultaneously produces macropores to allow the diffusion of the virus. However, challenging aspects of molecularly imprinted polymers for virus recognition, and more generally proteins, in bulk, such as template removal and rebinding, integrity of the binding sites, and random organization of the AuNP makes reproducibility more difficult to achieve without a precise optimization of the system towards each parameter (AuNP concentration, virus stability, etc.). This aspect should be studied more in details for future application. Also, the high number of viruses needed to get a response still represents a limitation for real life applications, but our aim was to provide a first proof into the ability of responsive hydrogels to recognize viruses by changing in color and size.

Conflicts of interest

There are no conflicts to declare.

Acknowledgments

We thank Cathleen Schlesener (Freie Universität of Berlin) for the synthesis of dendritic polyglycerol and the assistance of the Core Facility BioSupraMol supported by the DFG. We also thank the Helmholtz Graduate School MacroBio for the financial support and Dr. Pamela Winchester for language polishing the manuscript.

References

1. A. N. Wilson and A. Guiseppi-Elie, *Advanced Healthcare Materials*, 2013, **2**, 520-532.
2. R. V. Ulijn, N. Bibi, V. Jayawarna, P. D. Thornton, S. J. Todd, R. J. Mart, A. M. Smith and J. E. Gough, *Materials Today*, 2007, **10**, 40-48.
3. Y.-L. Wu, X. Chen, W. Wang and X. J. Loh, *Macromolecular Chemistry and Physics*, 2016, **217**, 175-188.
4. Y. Lu, A. A. Aimetti, R. Langer and Z. Gu, *Nature Reviews Materials*, 2016, **2**, 16075.
5. T. Miyata, N. Asami and T. Uragami, *Nature*, 1999, **399**, 766-769.
6. T. Miyata, T. Uragami and K. Nakamae, *Advanced Drug Delivery Reviews*, 2002, **54**, 79-98.
7. T. Miyata, A. Jikihara, K. Nakamae and A. S. Hoffman, *Macromolecular Chemistry and Physics*, 1996, **197**, 1135-1146.
8. T. Miyata, N. Asami and T. Uragami, *Macromolecules*, 1999, **32**, 2082-2084.
9. W. Bai and D. A. Spivak, *Angewandte Chemie International Edition*, 2014, **53**, 2095-2098.
10. J.-P. Couturier, M. Sütterlin, A. Laschewsky, C. Hettrich and E. Wischerhoff, *Angewandte Chemie International Edition*, 2015, **54**, 6641-6644.
11. J. E. Song and E. C. Cho, *Scientific Reports*, 2016, **6**, 34622.
12. M. I. Polymers, *Techniques and Instrumentation in Analytical Chemistry*, 2001, **23**.
13. F. L. Dickert and O. Hayden, *Analytical Chemistry*, 2002, **74**, 1302-1306.
14. T. Miyata, M. Jige, T. Nakaminami and T. Uragami, *Proceedings of the National Academy of Sciences*, 2006, **103**, 1190.
15. M. E. Byrne and V. Salian, *International journal of pharmaceutics*, 2008, **364**, 188-212.
16. G. Pan, S. Shinde, S. Yeung, M. Jakštaitė, Q. Li, A. Wingren and B. Sellergren, *An Epitope-Imprinted Biointerface with Dynamic Bioactivity for Modulating Cell-Biomaterial Interactions*, 2017.
17. W. Chen, Y. Ma, J. Pan, Z. Meng, G. Pan and B. Sellergren, *Polymers*, 2015, **7**, 1689-1715.
18. P. Thoniyot, M. J. Tan, A. A. Karim, D. J. Young and X. J. Loh, *Advanced Science*, 2015, **2**, 1400010.
19. R. Randriantsilefisoa, J. L. Cuellar-Camacho, M. S. Chowdhury, P. Dey, U. Schedler and R. Haag, *Journal of Materials Chemistry B*, 2019, DOI: 10.1039/C9TB00234K.
20. J. E. Stencel-Baerenwald, K. Reiss, D. M. Reiter, T. Stehle and T. S. Dermody, *Nat Rev Microbiol*, 2014, **12**, 739-749.
21. I. Papp, C. Sieben, K. Ludwig, M. Roskamp, C. Böttcher, S. Schlecht, A. Herrmann and R. Haag, *Small*, 2010, **6**, 2900-2906.
22. C. Lee, M. A. Gaston, A. A. Weiss and P. Zhang, *Biosensors & bioelectronics*, 2013, **42**, 236-241.
23. Y.-C. Yeh, B. Creran and V. M. Rotello, *Nanoscale*, 2012, **4**, 1871-1880.

Supporting Information

Double Trouble for Viruses: Hydrogel Nanocomposite Catches Influenza Virus While Shrinking and Changing Color

Rotsiniaina Randriantsilefisoa, Chuanxiong Nie, Badri Parshad, Yuanwei Pan, Sumati Bhatia and Rainer Haag**

Institut für Chemie und Biochemie, Freie Universität Berlin, Takustr. 3, 14195 Berlin, Germany

E-mail: haag@chemie.fu-berlin.de, rani2f@zedat.fu-berlin.de

Materials and Methods

All chemicals were purchased from Sigma (Germany) and used without further purification, unless otherwise noted. α-Amino-ω-azido PEG, PEG-MW. 3000 Dalton was purchased from RAPP Polymer (Germany). Dendritic polyglycerol cyclooctyne (dPG-C) with a number average molecular weight (Mn) of 10,000 Dalton and polyethylene glycol derivatives were synthesized as previously reported.[1]

Gold Nanoparticle Synthesis and Sialic Acid Conjugation

The synthesis of AuNP (20 nm) conjugated with sialic acid was performed as previously reported.[2] Briefly, 10 ml of 1.25 mM sialic acid was prepared in distilled water and mixed with an aqueous solution of $HAuCl_4$ (0.005 M, 1 ml) was brought to reflux at 80 °C at constant stirring at 1200 rpm for 20 min. The color of the solution changed from clear/yellow to light red wine. The suspension was then allowed to cool to room temperature. After that, the suspension (1 mL) was centrifuged for 10 min at 13,000 rpm. The supernatant was removed and the sediment redispersed in distilled water (1 mL).

UV-Visible characterization of AuNP-SA

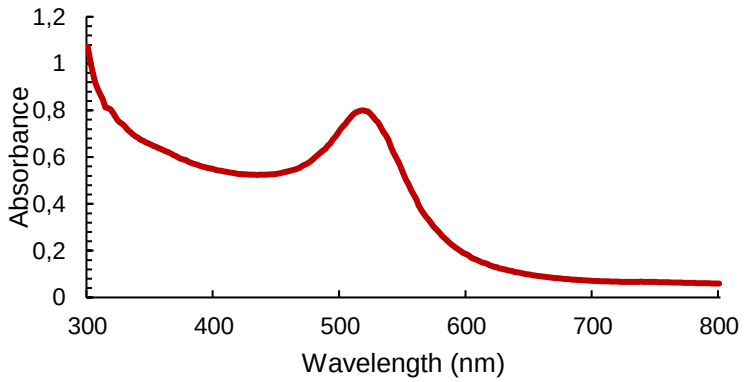

Figure S1. UV-vis spectra of AuNP-SA displaying a plasmon shift at λ = 525 nm.

Infrared (IR) spectrum of AuNP-SA

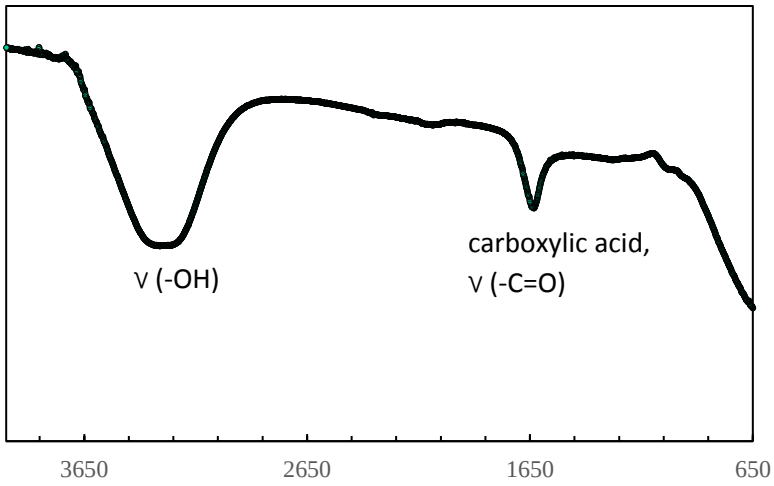

Figure S2. IR spectra of conjugated sialic acid AuNP.

A/X31 (H3N2) Virus Detection in Solution

Stock solutions of Influenza virus A/X31 (H3N2) ($1.2 * 10^9$ pfu/ml, 0.31 mg/mL protein) was prepared in 10 mM PBS and diluted into the concentrations of $4 * 10^8$, $2 * 10^8$, $1 * 10^8$, $5 * 10^7$, $1 * 10^7$, and 0 pfu/ml. The previous final solutions of AuNP-SA were added into the viruses solutions at equal volume (100 µL each). After being incubated for 30 min at 37°C, the color is recorded by a digital camera and quantified by UV-Vis spectra. . As a control for specificity, to the previous final solutions of SA-AuNP were added an unspecific protein solution (0.22 mg/ml proteins of VSV virus). The obtained solution did not undergo any color change. The color difference or indifference was quantified by UV-Vis measurements using a plate reader.

Specificity in Solution

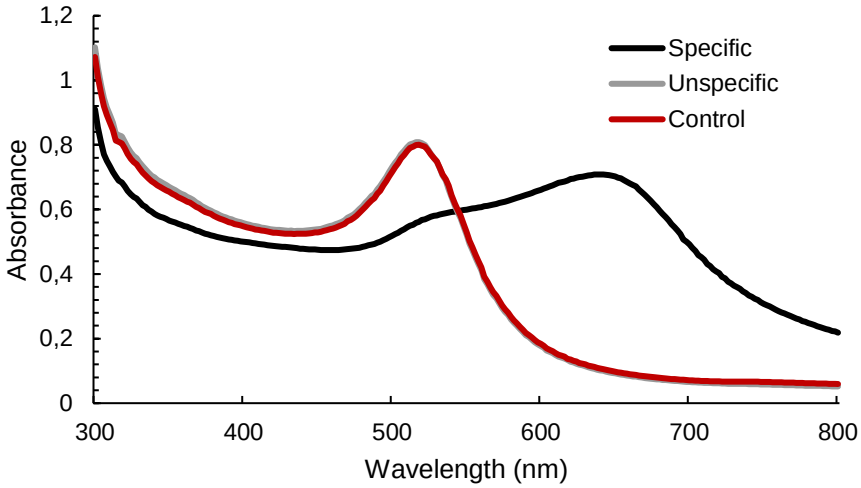

Figure S3. UV-vis spectrum of SA-AuNP solution with specific or unspecific viruses to sialic acid showing the absence of interaction of the SA-AuNP with VSV virus but only with A/X31 (H3N2) IAV. The control was plain SA-AuNP solution with PBS.

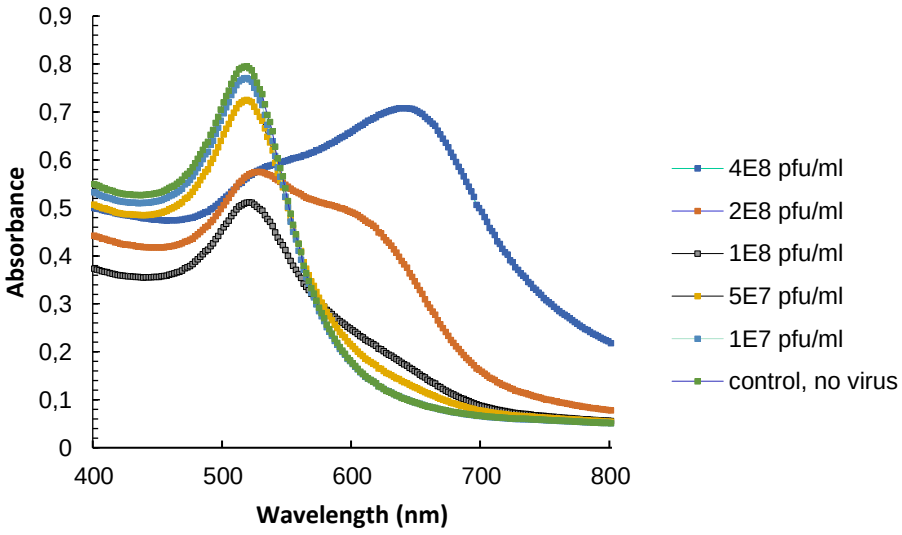

Figure S4. UV-vis spectrum of SA-AuNP solution with specific IAV A/X31 (H3N2) to sialic acid, with different concentrations of viruses. The control was plain SA-AuNP solution with PBS.

Preparation of Hydrogels for Virus Detection

Gold Nanoparticle Synthesis and Sialic Acid Conjugation for Hydrogels

The synthesis of AuNP (20 nm) conjugated with sialic acid was performed as previously reported with some modifications. Briefly, 10 ml of 1.25 mM sialic acid was prepared in distilled water and mixed with an aqueous solution of $HAuCl_4$ (0.005 M, 1 ml) was brought to reflux at 80 °C at constant stirring at 1200 rpm for 20 min. The color of the solution changed from clear/yellow to light red wine. The suspension was then allowed to cool to room temperature. After that, the suspension (1 ml) was centrifuged for 10 min at 13000 rpm. The supernatant was removed and the sediment redispersed in distilled water (200 µl) to obtain an intense red wine color.

Hydrogels and Bioimprinting Process

Prior to hydrogel formation, to the previous solution of Au-SA-virus conjugates (100 µl, $5 * 10^7$ pfu/ml) were added thiolated-PEG-diazide (10 mg) to get a concentration of 10 wt% PEG solution. The reaction mixture was left 30 min at rt to allow the thiol groups to bind to the AuNPs conjugates.

To this mixture of Au-SA-virus-PEG-diazide was added 125 wt% dPG-cyclooctyne and the bio-imprinted hydrogel was formed by mixing both components at a 2:10 ratio dPG: PEG. 10 µL of the mixture was added to small Eppendorf tubes to afford the final hydrogels with consistent shapes. The hydrogels were formed quickly after a few minutes. This group is called molecularly imprinted polymers “MIP.”

As a control group, hydrogels were formed the same way but without virus templates and were called non-imprinted polymers “NIP.”

Removal of Viruses

To mold the virus imprint into the hydrogel, the previously bound virus was removed by immersing the hydrogels in a big volume of stirring solution of 3.7 % hydrochloric acid (~ 100 ml) for two days. After reaching equilibrium, the hydrogels were washed in distilled water overnight. These samples were called “MDP.”.

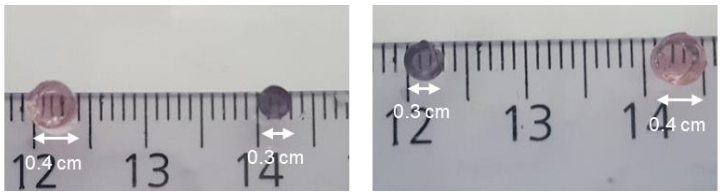

Figure S5. Photographs of hydrogels with and without virus template. Pink are the hydrogels bio-imprinted during the virus template removal process. Purple are the hydrogels with virus template (before template removal). Hydrogels without template already expanded by ~ 33 % in size after a few hours in 3.7 % HCl compared to the hydrogels with template in distilled water.

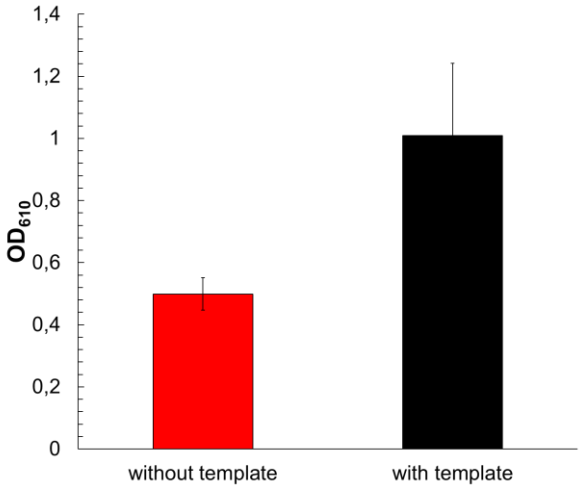

Figure S6. Optical density of hydrogels bio-imprinted after virus template removal (“without template”) and hydrogel with virus template (“with template”) at 610 nm.

Rebinding of Virus

Rebinding of virus was performed by immersing the nanocomposite bio-imprinted hydrogels into 10 µl of 1.2 * 10^9 pfu/ml (0.31 mg/ml HA) overnight.

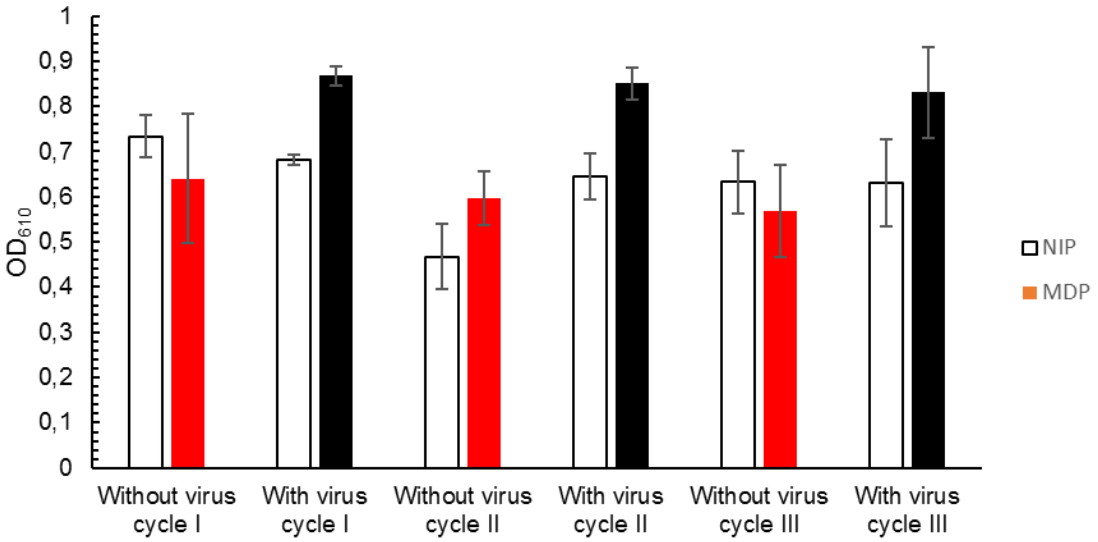

Figure S7. OD_{610} of hydrogels for different cycles of binding/removal of A/X31 (H3N2) virus in MDP and NIP for different hydrogels with incorporated p-values showing that imprinting was necessary to get the hydrogel response.

Specificity in Hydrogels

To assess the specificity, a nanocomposite bio-imprinted hydrogel was immersed into a solution containing unspecific virus (VSV virus, 0.22 mg/ml proteins).

References

1. R. Randriantsilefisoa, Y. Hou, Y. Pan, J. L. C. Camacho, M. W. Kulka, J. Zhang and R. Haag, *Advanced Functional Materials*, 2019.
2. C. Lee, M. A. Gaston, A. A. Weiss and P. Zhang, *Biosensors & bioelectronics*, 2013, **42**, 236-241.

5 Summary and Conclusions

The need for new designs of biomaterials for existing challenges in biomedical applications has led to the fabrication of three different polymeric hydrogels using dendritic polyglycerol and polyethylene glycol. These polymers were used for their bio-inertness, the possibility of a large varieties of functionalization and the ability to adapt the mechanical properties of the resulting material to the desired applications.

In the first project, the aim was to build a bioactive material specific for antibody detection where specific peptides were immobilized in the matrix as capture ligands. The challenge was to immobilize these molecules of recognition without altering their biological functions, without any change of conformation nor denaturation and without any leaching out of the system overtime. The easy and fast crosslinking biorthogonal approach to build the hydrogels was therefore well suited for the biosensing applications since they were also customizable to the desired application. The main reason for the use of hydrogels was to enhance the capability of 3D structures to improve biosensing strategies in terms of sensitivity, high loading capacity, and stability of the biomolecules, which prevents errors in the sensing method. Another aspect was the possibility of miniaturization of the system by using, for example, microarrays. All these aspects lack in existing 2D systems, which are however used in current biosensors. The strategy was thus to improve these existing 2D systems by using the advantages offered by a 3D hydrogel approach.

To predict the biosensing ability of our systems, we first characterized in depth the hydrogels in nano- and micro-scales, varying the molecular weights of the linkers. The linkers would influence the mechanical properties and morphology of the hydrogel networks. Regarding the physical properties of the networks, a remarkable swelling of the hydrogels (up to 100 their dry weight) was reached with an increasing swelling as a function of the molecular weights of the linkers. For the biosensing characterization, we obtained a specific and selective detection. Besides, a higher loading capacity was obtained with seven times higher than the one of 2D arrays. The sensitivity increased by 20% compared to the 2D detection method, the obtained limit of detection being 27 pg/mL.

In the second project, we proposed a patterned soft nanocomposite hydrogel as a soft cell culture scaffold. Directing stem cells to a specific lineage and keeping their pluripotency is challenging. And yet, in soft tissue engineering, soft tissue reconstruction to restore deficient tissues underneath the skin remains a hard endeavor. Recent studies have shown that culturing

hMSCs on typical TCPS or glass (hard substrates) has damaged the intrinsic function of these cells which has led to loss of stemness as the number of passages increased. In addition, they lost their adipogenesis differentiation potential. Stemness is defined as the mechano-sensing ability, immunophenotyping, and differentiation potential of a cell. To retain these properties of the stem cell, we produced a tissue mimicking cell-responsive platform by tuning the mechanical, biological, and morphological characteristics of the nanocomposite fabricated in a biorthogonal click strategy and Au-S chemistry. We obtained nanocomposites with stiffness in the range of liver tissues (elastic moduli < 2 kPa). To correctly predict the effect of the matrix on hMSCs, we studied their mechanical properties as a function of two different molecular weights of PEG linkers. The locomotion of hMSCs was first investigated on two different surfaces with patterns (wrinkles or creases) and the strong attachment of the cells on the nanocomposites was assessed. Stemness and differentiation potential were observed with an influence of the mechanical characteristics and the presence of adhesive peptides (RGD) and their spatial organization. We hypothesized that such system would influence the cells' behavior and morphology. In addition, they would keep their stemness compared to on bare TCPS or glass (hard surfaces). The studies have shown that a cell culture on these hydrogels preserved the immunophenotyping and mechano-sensibility of the hMSCs but lost on hard surfaces. This suggested that these polymeric networks had a positive influence on the hMSCs' fate by keeping their pluripotency. Finally, the soft substrates allowed exclusively the differentiation into a specific lineage, yielding adipocytes.

In the third project, a hybrid hydrogel has been established using both inorganic and organic materials to produce a nanocomposite. The hydrogel was virus responsive giving a double response, both an optical and a mechanical response to Influenza virus. We combined the use of gold nanoparticles for their optical properties, polysaccharides (sialic acid) for their specificity to Influenza virus and polyols for their ability to produce a highly swellable hydrogel. Besides the unique optical properties of gold nanoparticles displaying a color change visible by naked eyes, they also offer the possibility to anchor multiple molecules and biomolecules preventing at the same time any leaching out of the network and a better stability. The polyols (polyethylene glycol and dendritic polyglycerol) produced a bio-orthogonal hydrogel by strain-promoted azide-alkyne cycloaddition, which represents a suitable environment for biospecies by preventing their denaturation and any unspecific interaction. In addition, to enhance the specificity of the system, we used a bioimprinting procedure and used the virus as a template to create specific recognition sites. Specific recognition of macro-

biomolecules such as virus represents a challenge and a responsive system giving a double response to viruses is unique to this date. We present here a proof-of-principle that any virus and more generally any multivalent molecule can be recognized in a responsive polymer network by responding with a color change and shrinkage detectable by eyes. Given the specific molecules and imprint technique, these hydrogel features make it a customizable network for the desired application.

6 Kurzzusammenfassung

Die Herausforderungen im Bereich der Biomaterialie hat zur Entwicklung von drei verschiedenen Hydrogelen geführt, die in dieser Arbeit auf Basis von dendritischem Polyglycerin und Polyethylenglykol hergestellt wurden. Diese Polymere wurden aufgrund ihrer Bioverträglicheit, der Möglichkeit einer variablen Funktionalisierung und der Fähigkeit, die mechanischen Eigenschaften des resultierenden Materials auf die gewünschten Anwendungen abzustimmen, ausgewählt.

Im ersten Projekt war es das Ziel, ein bioaktives Material zu entwickeln, das spezifisch für den Antikörpernachweis reagiert, in dem Peptide in einer Matrix als Fänger-Liganden immobilisiert werden. Die Herausforderung besteht darin, die Peptide zu immobilisieren, ohne ihre biologischen Funktionen zu verändern durch Konformationsänderung, Denaturierung oder Auswaschen aus dem System. Der schnell vernetzende bio-orthogonale Ansatz zum Aufbau der Hydrogele war daher für die Biosensorik gut geeignet, da er auch an die gewünschte Anwendung angepasst werden konnte. Hierbei wurden Hydrogele eingesetzt, um 3D-Strukturen für Biosensorik-Strategien zu entwickeln und diese in ihrer Empfindlichkeit, Belastbarkeit und Stabilität zu optimieren, da diese Faktoren zu Fehlern in der Messmethode führen können. Ein weiterer Aspekt ist die Möglichkeit der Miniaturisierung des Systems, z.B. durch den Einsatz von Microarrays. All diese Aspekte fehlen in bestehenden 2D-Systemen, die jedoch in gegenwärtige Biosensore eingesetzt werden. Das Ziel dieser Arbeit besteht darin, die bestehenden 2D-Systeme durch die Vorteile eines 3D-Hydrogel Ansatzes zu verbessern.

Um die Biosensorfähigkeit unserer Systeme zu ermitteln, charakterisieren wir zunächst die Hydrogele im Nano- und Mikromaßstab in Abhängigkeit von vier verschiedenen Molekulargewichten der Linker, die die mechanischen Eigenschaften und die Morphologie solcher Materialien beeinflussen. Die Hydrogele zeigen ein bemerkenswertes Quellvermögen um den Faktor 100 und ein Höhenausdehnungsverhältnis um den Faktor 8. Für die Biosensorcharakterisierung erhielten wir ein spezifisches und selektives 3D-Detektionsmodell mit einer siebenmal höheren Belastbarkeit im Vergleich zu 2D-Arrays, einer höheren Empfindlichkeit von 20 % und einer Nachweisgrenze von bis zu 27 pg/ml.

Im zweiten Projekt haben wir ein strukturiertes, weiches Nanokomposit-Hydrogel als Grundgerüst für Gewebekulturen vorgeschlagen. Stammzellen auf eine bestimmte Entwicklungslinie zu lenken und dabei ihre Pluripotenz zu erhalten, ist eine Herausforderung. Dennoch bleibt die Wiederherstellung kaputten Gewebes unter der Haut eine schweringe

Aufgabe. Neuere Studien haben gezeigt, dass die Kultivierung von hMSCs auf typischen TCPS oder Glas (Hartsubstraten) die intrinsischen Funktionen dieser Zellen beschädigt. Was mit zunehmender Anzahl der Durchgänge zu einem Verlust der Stammzellfähigkeit führt. Darüber hinaus verlieren die Zellen ihr Differenzierungspotenzial in der Adipogenese. Die Stammzellfähigkeit ist definiert als mechano-sensor-Fähigkeit, Immunphänotypisierung und Differenzierungspotenzial. Um diese Eigenschaften der Zellen zu erhalten, haben wir eine gewebeähnliche, zellreaktive Plattform entwickelt. Diese ist definiert durch die mechanischen und morphologischen Eigenschaften des Hydrogels, welches in einer bio-orthogonalen Klickstrategie und Au-S-Chemie hergestellt wird. Wir erhielten Nanokomposite mit der Steifheit im Bereich von Lebergewebe (< 2 kPa). Um den Einfluss der Matrix auf hMSCs zu ermitteln, haben wir die mechanischen Eigenschaften der Hydrogele als Funktion von zwei verschiedenen Molekulargewichten von PEG-Linkern untersucht. Nach der Untersuchung der Fortbewegung von hMSCs auf zwei unterschiedlich gemusterten Oberflächen (*wrinkled* oder *creased*) und der Beurteilung der starken Bindung von hMSCs an die Hydrogele wurden Stammzellfähigkeit und Differenzierungspotenzial mit einem Einfluss der Veränderung der mechanischen Eigenschaften und der Organisation des adhäsiven Peptids (RGD) bestätigt. Wir haben angenommen, dass solche Systeme das Verhalten und die Morphologie der Zellen beeinflussen würden und dass sie ihre Steifheit im Vergleich zu unbeschichtetem TCPS oder Glas (harte Oberflächen) beibehalten würden. Die Ergebnisse haben gezeigt, dass die Immunphänotypisierung und Mechanosensitivität der hMSCs auf diesen Hydrogelen erhalten bleibt und beim Anbau auf harten Oberflächen verloren geht. Dies deutet darauf hin, dass diese Hydrogele einen positiven Einfluss auf die Entwicklung der hMSCs haben, da sie ihre Pluripotenz erhalten. Zudem führten die weichen Substrate ausschließlich zur Differenzierung in eine bestimmte Linie, wodurch Adipozyten entstanden.

Im dritten Projekt wurde ein Hybrid-Hydrogel etabliert, das sowohl anorganische als auch organische Materialien zur Herstellung eines Nanokomposits beinhaltet. Das Hydrogel erzeugt eine optische als auch eine mechanische Reaktion auf das Influenzavirus. Wir kombinieren die Verwendung von Goldnanopartikeln für ihre optischen Eigenschaften, Polysaccharide (Sialinsäure) für die Spezifität auf das Influenzavirus und Polyole um ein Hydrogel zu erzeugen. Neben den optischen Eigenschaften von Goldnanopartikeln, die eine mit bloßem Auge sichtbare Farbveränderung aufweisen, bieten sie auch die Möglichkeit, mehrere Moleküle und Biomoleküle zu verankern, um ein Austreten aus dem Netzwerk zu verhindern und die Stabilität zu erhöhen. Die Polyole (Polyethylenglykol und dendritisches Polyglycerin)

reagieren durch Azid-Alkyn-Cycloaddition zu einem bio-orthogonalen Hydrogel, welches eine geeignete Umgebung für Biospezies darstellt, indem es deren Denaturierung und unspezifische Wechselwirkungen verhindert. Um die Spezifität des Systems zu erhöhen, haben wir ein Bioimprinting-Verfahren verwendet und das Virus als Maske verwendet, um spezifische Erkennungsstellen zu erzeugen. Die spezifische Erkennung von Makro-Biomolekülen, wie einem Virus, stellt eine Herausforderung dar. Und ein reaktionsschnelles System, das auf Viren doppelt reagiert, ist bis heute einzigartig. Wir stellen hier einen Nachweis des funktionierenden Prinzips vor, in dem Viren oder andere multivalente Moleküle in einem Polymernetzwerk schnell erkannt werden können. Dieses Polymernetzwerk reagiert darauf durch Farbänderung und Volumenverkleinerung, die mit bloßem Augen erkannt werden kann. Aufgrund der spezifischen Molekülinteraktion und der Imprint-Technik sind diese Hydrogele ein variables System für passende Sensor-Anwendungen.

7 References

[1] S. D. B. K. N. V. N. Kanchi S, *Journal of Environmental Analytical Chemistry* **2015**, *2*, 1-4.

[2] aM. Cuzin, *Transfusion clinique et biologique : journal de la Societe francaise de transfusion sanguine* **2001**, *8*, 291-296; bG.-P. Nikoleli, C. G. Siontorou, D. P. Nikolelis, S. Bratakou, S. Karapetis, N. Tzamtzis, in *Nanotechnology and Biosensors* (Eds.: D. P. Nikolelis, G.-P. Nikoleli), Elsevier, **2018**, pp. 375-394; cJ. Noh, H. C. Kim, T. D. Chung, *Topics in current chemistry* **2011**, *304*, 117-152; dP. Hong, W. Li, J. Li, *Sensors (Basel)* **2012**, *12*, 1181-1193; eA. Kaushik, A. Yndart, S. Kumar, R. D. Jayant, A. Vashist, A. N. Brown, C.-Z. Li, M. Nair, *Scientific Reports* **2018**, *8*, 9700; fD. Kinnamon, R. Ghanta, K.-C. Lin, S. Muthukumar, S. Prasad, *Scientific Reports* **2017**, *7*, 13312; gJ. Kim, A. S. Campbell, B. E.-F. de Ávila, J. Wang, *Nature Biotechnology* **2019**, *37*, 389-406.

[3] G. A. Urban, T. Weiss, in *Hydrogel Sensors and Actuators: Engineering and Technology* (Eds.: G. Gerlach, K.-F. Arndt), Springer Berlin Heidelberg, Berlin, Heidelberg, **2010**, pp. 197-220.

[4] F. Rusmini, Z. Zhong, J. Feijen, *Biomacromolecules* **2007**, *8*, 1775-1789.

[5] aT. R. Hoare, D. S. Kohane, *Polymer* **2008**, *49*, 1993-2007; bJ. Y. Seo, B. Lee, T. W. Kang, J. H. Noh, M. J. Kim, Y. B. Ji, H. J. Ju, B. H. Min, M. S. Kim, *Tissue Engineering and Regenerative Medicine* **2018**, *15*, 513-520; cA. S. Hoffman, *Advanced Drug Delivery Reviews* **2012**, *64*, 18-23; dE. Caló, V. V. Khutoryanskiy, *European Polymer Journal* **2015**, *65*, 252-267; eD. Seliktar, *Science (New York, N.Y.)* **2012**, *336*, 1124; fN. A. Peppas, D. S. Van Blarcom, *Journal of Controlled Release* **2016**, *240*, 142-150.

[6] Q. Chai, Y. Jiao, X. Yu, *Gels (Basel, Switzerland)* **2017**, *3*, 6.

[7] B. Morteza, M. Naimeh, M. Mehdi, **2016**.

[8] aE. Bender, *Nature* **2016**, *540*, S106; bD. Howard, L. D. Buttery, K. M. Shakesheff, S. J. Roberts, *J Anat* **2008**, *213*, 66-72; cL. Benning, L. Gutzweiler, K. Tröndle, J. Riba, R. Zengerle, P. Koltay, S. Zimmermann, G. B. Stark, G. Finkenzeller, *Journal of Biomedical Materials Research Part A* **2017**, *105*, 3231-3241; dE. Sykova, S. Forostyak, *Laser Ther* **2013**, *22*, 87-92.

[9] T. E. Ludwig, A. Kujak, A. Rauti, S. Andrzejewski, S. Langbehn, J. Mayfield, J. Fuller, Y. Yashiro, Y. Hara, A. Bhattacharyya, *Cell stem cell* **2018**, *23*, 644-648.

[10] aJ.-H. Lee, H.-W. Kim, *J Tissue Eng* **2018**, *9*, 2041731418768285-2041731418768285; bI. M. El-Sherbiny, M. H. Yacoub, *Glob Cardiol Sci Pract* **2013**, *2013*, 316-342; cJ. A. Hunt, R. Chen, T. van Veen, N. Bryan, *Journal of Materials Chemistry B* **2014**, *2*, 5319-5338; dM. Liu, X. Zeng, C. Ma, H. Yi, Z. Ali, X. Mou, S. Li, Y. Deng, N. He, *Bone Research* **2017**, *5*, 17014; eS. Ahadian, H. Savoji, A. Khademhosseini, *Recent Advances in Hydrogels for Tissue Engineering, Vol. 114*, **2018**.

[11] F. Ganji, S. Vasheghani Farahani, E. Vasheghani-Farahani, *Theoretical Description of Hydrogel Swelling: A Review, Vol. 19*, **2010**.

[12] N. Chirani, L. H. Yahia, L. Gritsch, F. Motta, S. Chirani, S. Farè, *History and Applications of Hydrogels, Vol. Vol. 4*, **2015**.

[13] aO. Wichterle, D. LÍM, *Nature* **1960**, *185*, 117-118; bS. Lin, X. Liu, J. Liu, H. Yuk, H.-C. Loh, G. A. Parada, C. Settens, J. Song, A. Masic, G. H. McKinley, X. Zhao, *Science Advances* **2019**, *5*, eaau8528; cL. Li, F. Yu, L. Zheng, R. Wang, W. Yan, Z. Wang, J. Xu, J. Wu, D. Shi, L. Zhu, X. Wang, Q. Jiang, *Journal of Orthopaedic Translation* **2018**; dJ.-Y. Sun, X. Zhao, W. R. K. Illeperuma, O. Chaudhuri, K. H. Oh, D. J. Mooney, J. J. Vlassak, Z. Suo, *Nature* **2012**, *489*, 133; eJ. Kopecek, *Biomaterials* **2007**, *28*, 5185-5192.

[14] aK. Varaprasad, G. M. Raghavendra, T. Jayaramudu, M. M. Yallapu, R. Sadiku, *Materials Science and Engineering: C* **2017**, *79*, 958-971; bF. Ullah, M. B. H. Othman, F. Javed, Z. Ahmad, H. M. Akil, *Materials Science and Engineering: C* **2015**, *57*, 414-433.

[15] R. E. Rivero, F. Alustiza, N. Rodríguez, P. Bosch, M. C. Miras, C. R. Rivarola, C. A. Barbero, *Reactive and Functional Polymers* **2015**, *97*, 77-85.

[16] aM. Ahmad, S. M. Rai, A. Mahmood, *Advances in Polymer Technology* **2016**, *35*, 121-128; bN. Mushi, J. Kochumalayil, N. Cervin, Q. Zhou, L. Berglund, *Nanostructurally Controlled Hydrogel Based on Small-Diameter Native Chitin Nanofibers: Preparation, Structure, and Properties, Vol. 9*, **2016**; cA. Barbetta, G. Rizzitelli, R. Bedini, R. Pecci, M. Dentini, *Soft Matter* **2010**, *6*, 1785-1792.

[17] L. J. Del Valle, A. Diaz, J. Puiggali, *Gels (Basel, Switzerland)* **2017**, *3*.

[18] F. Redaelli, M. Sorbona, F. Rossi, in *Bioresorbable Polymers for Biomedical Applications* (Eds.: G. Perale, J. Hilborn), Woodhead Publishing, **2017**, pp. 205-228.

[19] R. A. McBath, D. A. Shipp, *Polymer Chemistry* **2010**, *1*, 860-865.

[20] F. Liu, J. Seuring, S. Agarwal, *Macromolecular Chemistry and Physics* **2014**, *215*, 1466-1472.

[21] C. R. Mayer, R. Thouvenot, T. Lalot, *Macromolecules* **2000**, *33*, 4433-4437.

[22] M. Zhou, K. Liu, X. Qian, *Journal of Applied Polymer Science* **2016**, *133*.

[23] L. H. Sperling, in *Interpenetrating Polymer Networks, Vol. 239*, American Chemical Society, **1994**, pp. 3-38.

[24] E. S. Dragan, *Chemical Engineering Journal* **2014**, *243*, 572-590.

[25] N. Sivagangi Reddy, K. Madhusudana Rao, T. J. Sudha Vani, K. S. V. Krishna Rao, Y. I. Lee, *Desalination and Water Treatment* **2016**, *57*, 6503-6514.

[26] E. M. Ahmed, *Journal of Advanced Research* **2015**, *6*, 105-121.

[27] S. Yigit, R. Sanyal, A. Sanyal, *Chemistry – An Asian Journal* **2011**, *6*, 2648-2659.

[28] C. A. Deforest, E. A. Sims, K. S. Anseth, *Chem Mater* **2010**, *22*, 4783-4790.

[29] C. A. DeForest, K. S. Anseth, *Nature Chemistry* **2011**, *3*, 925.

[30] D. P. Nair, M. Podgórski, S. Chatani, T. Gong, W. Xi, C. R. Fenoli, C. N. Bowman, *Chemistry of Materials* **2014**, *26*, 724-744.

[31] E. H. Cordes, W. P. Jencks, *Journal of the American Chemical Society* **1962**, *84*, 832-837.

[32] N. L. Morozowich, J. L. Nichol, H. R. Allcock, *Journal of Polymer Science Part A: Polymer Chemistry* **2016**, *54*, 2984-2991.

[33] T. Hozumi, T. Kageyama, S. Ohta, J. Fukuda, T. Ito, *Biomacromolecules* **2018**, *19*, 288-297.

[34] L. J. Macdougall, V. X. Truong, A. P. Dove, *ACS Macro Letters* **2017**, *6*, 93-97.

[35] V. T. Huynh, G. Chen, P. d. Souza, M. H. Stenzel, *Biomacromolecules* **2011**, *12*, 1738-1751.

[36] S. Singh Gujral, **2013**.

[37] L. J. Smith, S. M. Taimoory, R. Y. Tam, A. E. G. Baker, N. Binth Mohammad, J. F. Trant, M. S. Shoichet, *Biomacromolecules* **2018**, *19*, 926-935.

[38] S.-Y. Choh, D. Cross, C. Wang, *Biomacromolecules* **2011**, *12*, 1126-1136.

[39] B. Gyarmati, Á. Némethy, A. Szilágyi, *European Polymer Journal* **2013**, *49*, 1268-1286.

[40] P. Calvert, P. Patra, D. Duggal, *Epoxy hydrogels as sensors and actuators, Vol. 6524*, SPIE, **2007**.

[41] D. Saraydın, E. Karadagˇ, Y. Işıkver, N. Şahiner, O. Güven, *Journal of Macromolecular Science, Part A* **2004**, *41*, 419-431.

[42] S. Khan, A. Ullah, K. Ullah, N.-u. Rehman, *Designed Monomers and Polymers* **2016**, *19*, 456-478.

[43] P. J. Flory, *Principles of polymer chemistry*, Cornell University Press, Ithaca, N.Y., **1953**.

[44] M. S. Rehmann, K. M. Skeens, P. M. Kharkar, E. M. Ford, E. Maverakis, K. H. Lee, A. M. Kloxin, *Biomacromolecules* **2017**, *18*, 3131-3142.

[45] M. Capurro, F. Barberis, in *Biomaterials for Bone Regeneration* (Eds.: P. Dubruel, S. Van Vlierberghe), Woodhead Publishing, **2014**, pp. 270-323.

[46] C. Tamerler, *JOM* **2015**, *67*, 2480-2482.

[47] aA. Vedadghavami, F. Minooei, M. H. Mohammadi, S. Khetani, A. Rezaei Kolahchi, S. Mashayekhan, A. Sanati-Nezhad, *Acta biomaterialia* **2017**, *62*, 42-63; bT. S. Hin, *Engineering Materials for Biomedical Applications*; cM. W. Tibbitt, C. B. Rodell, J. A. Burdick, K. S. Anseth, *Proceedings of the National Academy of Sciences of the United States of America* **2015**, *112*, 14444-14451; dM. M. Dewidar, H.-C. Yoon, J. K. Lim, *Metals and Materials International* **2006**, *12*, 193.

[48] P. Pàmies, A. Stoddart, *Nature Materials* **2013**, *12*, 957.

[49] aD. Caccavo, S. Cascone, G. Lamberti, A. A. Barba, *Chemical Society Reviews* **2018**, *47*, 2357-2373; bN. E. Ben Ammar, T. Saied, M. Barbouche, F. Hosni, M. n. Adel, M. Sen, *A comparative study between three different methods of hydrogel network characterization: effect of composition on the crosslinking properties using sol–gel, rheological and mechanical analyses*, **2017**.

[50] B. D. Ratner, *Journal of cardiovascular translational research* **2011**, *4*, 523-527.

[51] P. Thevenot, W. Hu, L. Tang, *Current topics in medicinal chemistry* **2008**, *8*, 270-280.

[52] R. Mihai, I. P. Florescu, V. Coroiu, A. Oancea, M. Lungu, *J Med Life* **2011**, *4*, 250-255.

[53] D. Taki Miladinov, S. Tomi , S. Stojanovi , J. Najdanovi , J. Filipovi , M. Trajanovi , S. Najman, *Materials Research* **2016**, *19*, 1070-1079.

[54] E. P. Ivanova, K. Bazaka, R. J. Crawford, in *New Functional Biomaterials for Medicine and Healthcare* (Eds.: E. P. Ivanova, K. Bazaka, R. J. Crawford), Woodhead Publishing, **2014**, pp. 71-99.

[55] S. Zalipsky, J. M. Harris, in *Poly(ethylene glycol), Vol. 680*, American Chemical Society, **1997**, pp. 1-13.

[56] C. Yesildag, Z. Ouyang, Z. Zhang, M. C. Lensen, *Frontiers in Chemistry* **2019**, *6*.

[57] J. A. Asenjo, B. A. Andrews, *Journal of chromatography. A* **2011**, *1218*, 8826-8835.

[58] D. Dutheil, A. Underhaug Gjerde, I. Petit-Paris, G. Mauco, H. Holmsen, *J Chem Biol* **2009**, *2*, 39-49.

[59] P. B. Lawrence, J. L. Price, *Curr Opin Chem Biol* **2016**, *34*, 88-94.

[60] aV. Hynninen, L. Vuori, M. Hannula, K. Tapio, K. Lahtonen, T. Isoniemi, E. Lehtonen, M. Hirsimäki, J. J. Toppari, M. Valden, V. P. Hytönen, *Scientific Reports* **2016**, *6*, 29324; bT. Ekblad, G. Bergström, T. Ederth, S. L. Conlan, R. Mutton, A. S. Clare, S. Wang, Y. Liu, Q. Zhao, F. D'Souza, G. T. Donnelly, P. R. Willemsen, M. E. Pettitt, M. E. Callow, J. A. Callow, B. Liedberg, *Biomacromolecules* **2008**, *9*, 2775-2783.

[61] N. Gjorevski, M. P. Lutolf, *Nature Protocols* **2017**, *12*, 2263.

[62] aK. Kinbara, *Polymer Journal* **2018**, *50*, 689-697; bA. A. D'souza, R. Shegokar, *Expert Opinion on Drug Delivery* **2016**, *13*, 1257-1275.

[63] aA. M. Ross, J. Lahann, *Annual Review of Chemical and Biomolecular Engineering* **2015**, *6*, 161-186; bM. Tanaka, T. Hayashi, S. Morita, *Polymer Journal* **2013**, *45*, 701.

[64] J. Smith, D. Lamprou, *Polymer coatings for biomedical applications: A review, Vol. 92*, **2014**.

[65] A. Sunder, R. Mülhaupt, R. Haag, H. Frey, *Hyperbranched Polyether Polyols: A Modular Approach to Complex Polymer Architectures, Vol. 12*, **2000**.

[66] A. Sunder, R. Hanselmann, H. Frey, R. Mülhaupt, *Macromolecules* **1999**, *32*, 4240-4246.

[67] aM. Calderon, M. A. Quadir, S. K. Sharma, R. Haag, *Advanced materials (Deerfield Beach, Fla.)* **2010**, *22*, 190-218; bE. Moore, H. Thissen, N. Voelcker, *Hyperbranched polyglycerols at the biointerface, Vol. 88*, **2013**.

[68] A. Nada, *Natural and Synthetic Biomedical Polymers*, **2014**.

[69] O. Olatunji, in *Natural Polymers: Industry Techniques and Applications* (Ed.: O. Olatunji), Springer International Publishing, Cham, **2016**, pp. 93-114.

[70] Q. Wei, N.-N. Deng, J. Guo, J. Deng, *Synthetic Polymers for Biomedical Applications, Vol. 2018*, **2018**.

[71] W. Xi, T. F. Scott, C. J. Kloxin, C. N. Bowman, *Advanced Functional Materials* **2014**, *24*, 2572-2590.

[72] V. V. Rostovtsev, L. G. Green, V. V. Fokin, K. B. Sharpless, *Angewandte Chemie International Edition* **2002**, *41*, 2596-2599.

[73] H. C. Kolb, M. G. Finn, K. B. Sharpless, *Angewandte Chemie International Edition* **2001**, *40*, 2004-2021.

[74] aD. A. Fulton, *Nature Chemistry* **2016**, *8*, 899; bK. L. Diehl, I. V. Kolesnichenko, S. A. Robotham, J. L. Bachman, Y. Zhong, J. S. Brodbelt, E. V. Anslyn, *Nature Chemistry* **2016**, *8*, 968.

[75] C. E. Hoyle, C. N. Bowman, *Angewandte Chemie International Edition* **2010**, *49*, 1540-1573.

[76] C. R. Becer, R. Hoogenboom, U. S. Schubert, *Angewandte Chemie International Edition* **2009**, *48*, 4900-4908.

[77] aD. N. Forthal, *Microbiol Spectr* **2014**, *2*, 1-17; bG. M. Edelman, *Science (New York, N.Y.)* **1973**, *180*, 830-840.

[78] D. R. Davies, S. Chacko, *Accounts of Chemical Research* **1993**, *26*, 421-427.

[79] G. B. Fields, *Curr Protoc Protein Sci* **2002**, *Chapter 18*, Unit-18.11.

[80] aR. B. Merrifield, *Journal of the American Chemical Society* **1963**, *85*, 2149-2154; bC. Petrou, Y. Sarigiannis, in *Peptide Applications in Biomedicine, Biotechnology and Bioengineering* (Ed.: S. Koutsopoulos), Woodhead Publishing, **2018**, pp. 1-21.

[81] B. Alberts, A. Johnson, J. Lewis, M. Raff, K. Roberts, P. Walter, in *Molecular Biology of the Cell. 4th edition*, Garland Science, **2002**.

[82] R. A. Edwards, F. Rohwer, *Nature Reviews Microbiology* **2005**, *3*, 504-510.

[83] T. Noda, *Frontiers in Microbiology* **2012**, *2*.

[84] S. J. Gamblin, J. J. Skehel, *J Biol Chem* **2010**, *285*, 28403-28409.

[85] aA. M. Weisner, H. Chart, A. Bush, J. C. Davies, T. L. Pitt, *Journal of medical microbiology* **2007**, *56*, 670-674; bK. Nishitani, C. A. Beck, A. F. Rosenberg, S. L. Kates, E. M. Schwarz, J. L. Daiss, *Clinical orthopaedics and related research* **2015**, *473*, 2735-2749.

[86] L. Wang, J. E. Filer, M. M. Lorenz, C. S. Henry, D. S. Dandy, B. J. Geiss, *Biosensors and Bioelectronics* **2019**, *131*, 46-52.

[87] A. Moody, *Clin Microbiol Rev* **2002**, *15*, 66-78.

[88] A. T. Kuna, L. Đerek, A. Kozmar, V. Drvar, *Biochem Med (Zagreb)* **2016**, *26*, 376-394.

[89] K. Johansen, L. Svensson, *Methods in molecular medicine* **1998**, *13*, 15-28.

[90] M. Kavuru, R. Tubbs, M. L. Miller, H. P. Wiedemann, *Immunocytometry and Gene Rearrangement Analysis in the Diagnosis of Lymphoma in an Idiopathic Pleural Effusion, Vol. 145*, **1992**.

[91] B. Magi, S. Liberatori, *Methods in molecular biology (Clifton, N.J.)* **2005**, *295*, 227-254.

[92] *Bull World Health Organ* **1976**, *54*, 129-139.

[93] J. Sobek, C. Aquino, W. Weigel, R. Schlapbach, *BMC Biophysics* **2013**, *6*, 8.

[94] S. B. Nimse, K. Song, M. D. Sonawane, D. R. Sayyed, T. Kim, *Sensors* **2014**, *14*, 22208.

[95] A. K. Trilling, J. Beekwilder, H. Zuilhof, *Analyst* **2013**, *138*, 1619-1627.

[96] aD. Kim, A. E. Herr, *Biomicrofluidics* **2013**, *7*, 041501; bA. D. Radadia, C. J. Stavis, R. Carr, H. Zeng, W. P. King, J. A. Carlisle, A. Aksimentiev, R. J. Hamers, R. Bashir, *Advanced Functional Materials* **2011**, *21*, 1040-1050.

[97] H. H. Garcia, Y. Castillo, I. Gonzales, J. A. Bustos, H. Saavedra, L. Jacob, O. H. Del Brutto, P. P. Wilkins, A. E. Gonzalez, R. H. Gilman, *Tropical Medicine & International Health* **2018**, *23*, 101-105.

[98] aE. Engvall, P. Perlmann, *Journal of immunology (Baltimore, Md. : 1950)* **1972**, *109*, 129-135; bP. J. Tighe, R. R. Ryder, I. Todd, L. C. Fairclough, *Proteomics. Clinical applications* **2015**, *9*, 406-422.

[99] aP. Mehrotra, *J Oral Biol Craniofac Res* **2016**, *6*, 153-159; bR. F. Taylor, I. G. Marenchic, R. H. Spencer, *Analytica Chimica Acta* **1991**, *249*, 67-70.

[100] M. Asal, Ö. Özen, M. Şahinler, H. T. Baysal, İ. Polatoğlu, *Sensor Review* **2019**, *39*, 377-386.

[101] C. G. J. Koopal, R. J. M. Nolte, *Enzyme and Microbial Technology* **1994**, *16*, 402-408.

[102] F. W. Scheller, F. Schubert, B. Neumann, D. Pfeiffer, R. Hintsche, I. Dransfeld, U. Wollenberger, R. Renneberg, A. Warsinke, G. Johansson, M. Skoog, X. Yang, V. Bogdanovskaya, A. Bückmann, S. Y. Zaitsev, *Biosensors and Bioelectronics* **1991**, *6*, 245-253.

[103] W. Zhang, G. Li, *Analytical sciences : the international journal of the Japan Society for Analytical Chemistry* **2004**, *20*, 603-609.

[104] C. I. L. Justino, T. A. Rocha-Santos, A. C. Duarte, T. A. Rocha-Santos, *TrAC Trends in Analytical Chemistry* **2010**, *29*, 1172-1183.

[105] M. Strianese, M. Staiano, G. Ruggiero, T. Labella, C. Pellecchia, S. D'Auria, *Methods in molecular biology (Clifton, N.J.)* **2012**, *875*, 193-216.

[106] J. Ji, W. Gu, C. Sun, J. Sun, H. Jiang, Y. Zhang, X. Sun, *Scientific Reports* **2016**, *6*, 31270.

[107] aJ. Lichtman, J. Conchello, *Fluorescence Microscopy, Vol. 2*, **2006**; bJ. R. Lakowicz, in *Principles of Fluorescence Spectroscopy* (Ed.: J. R. Lakowicz), Springer US, Boston, MA, **1999**, pp. 1-23.

[108] M. Narayanan Nair, **2013**.

[109] V. Dugas, A. Elaissari, Y. Chevalier, **2009**, pp. 47-134.

[110] S. Liébana, G. A. Drago, *Essays Biochem* **2016**, *60*, 59-68.

[111] S. B. Nimse, K. Song, M. D. Sonawane, D. R. Sayyed, T. Kim, *Sensors* **2014**, *14*, 22208-22229.

[112] B. Prieto-Simon, M. Campas, J. L. Marty, *Protein & Peptide Letters* **2008**, *15*, 757-763.

[113] G. MacBeath, S. L. Schreiber, *Science (New York, N.Y.)* **2000**, *289*, 1760-1763.

[114] D. Yeo, R. C Panicker, L.-P. Tan, S. Yao, *Strategies for Immobilization of Biomolecules in a Microarray, Vol. 7*, **2004**.

[115] aY. Fang, A. G Frutos, J. Lahiri, *Membrane Protein Microarrays, Vol. 124*, **2002**; bM. C. Sabra, J. C. Uitdehaag, A. Watts, *Biophys J* **1998**, *75*, 1180-1188; cM. Chadli, O. Maniti, C. Marquette, B. Tillier, S. Cortès, A. Girard-Egrot, *Analyst* **2018**, *143*, 2165-2173.

[116] aM. Meldal, S. Schoffelen, *F1000Res* **2016**, *5*, F1000 Faculty Rev-2303; bD. K. Kölmel, E. T. Kool, *Chemical Reviews* **2017**, *117*, 10358-10376; cC. D. Spicer, E. T. Pashuck, M. M. Stevens, *Chemical reviews* **2018**, *118*, 7702-7743.

[117] aX.-L. Sun, L. Yang, E. L. Chaikof, *Tetrahedron Lett* **2008**, *49*, 2510-2513; bM. N. Yousaf, M. Mrksich, *Journal of the American Chemical Society* **1999**, *121*, 4286-4287.

[118] aA. Watzke, M. Köhn, M. Gutierrez-Rodriguez, R. Wacker, H. Schröder, R. Breinbauer, J. Kuhlmann, K. Alexandrov, C. M Niemeyer, R. Goody, H. Waldmann, *Site-Selective Protein Immobilization by Staudinger Ligation, Vol. 45*, **2006**; bS. S. van Berkel, M. B. van Eldijk, J. C. M. van Hest, *Angewandte Chemie International Edition* **2011**, *50*, 8806-8827; cM. B. Soellner, K. A. Dickson, B. L. Nilsson, R. T. Raines, *Journal of the American Chemical Society* **2003**, *125*, 11790-11791.

[119] N. R. Mohamad, N. H. C. Marzuki, N. A. Buang, F. Huyop, R. A. Wahab, *Biotechnol Biotechnol Equip* **2015**, *29*, 205-220.

[120] aS. Cosnier, *Biosensors and Bioelectronics* **1999**, *14*, 443-456; bV. Kandimalla, V. Shyam Tripathi, H. Ju, *Immobilization of Biomolecules in Sol–Gels: Biological and Analytical Applications, Vol. 36*, **2006**.

[121] ain *Handbook of Biosensors and Biochips*; bW. Mattanavee, O. Suwantong, S. Puthong, T. Bunaprasert, V. P. Hoven, P. Supaphol, *ACS applied materials & interfaces* **2009**, *1*, 1076-1085.

[122] aC. L. O'Neil, K. J. Stine, A. V. Demchenko, *Journal of Carbohydrate Chemistry* **2018**, *37*, 225-249; bA. Malik, M. H. Baig, B. Manavalan, in *Encyclopedia of Bioinformatics and Computational Biology* (Eds.: S. Ranganathan, M. Gribskov, K. Nakai, C. Schönbach), Academic Press, Oxford, **2019**, pp. 666-677.

[123] F. E. Regnier, W. Cho, in *Proteomic and Metabolomic Approaches to Biomarker Discovery* (Eds.: H. J. Issaq, T. D. Veenstra), Academic Press, Boston, **2013**, pp. 197-224.

[124] aS. B. Nimse, K. Song, M. D. Sonawane, D. R. Sayyed, T. Kim, *Sensors (Basel)* **2014**, *14*, 22208-22229; bM. Wilchek, E. A. Bayer, *Analytical biochemistry* **1988**, *171*, 1-32; cM. Wilchek, E. A. Bayer, O. Livnah, *Immunology letters* **2006**, *103*, 27-32.

[125] R. V. Ulijn, N. Bibi, V. Jayawarna, P. D. Thornton, S. J. Todd, R. J. Mart, A. M. Smith, J. E. Gough, *Materials Today* **2007**, *10*, 40-48.

[126] aA. N. Wilson, A. Guiseppi-Elie, *Adv Healthc Mater* **2013**, *2*, 520-532; bT. Miyata, N. Asami, T. Uragami, *Nature* **1999**, *399*, 766-769.

[127] aR. V. Ulijn, N. Bibi, V. Jayawarna, P. Thornton, S. Todd, R. J. Mart, A. Smith, J. Gough, *Bioresponsive hydrogels, Vol. 10*, **2007**; bW. Chen, Y. Ma, J. Pan, Z. Meng, G. Pan, B. Sellergren, *Polymers* **2015**, *7*, 1689-1715.

[128] Y. Lu, A. A. Aimetti, R. Langer, Z. Gu, *Nature Reviews Materials* **2016**, *2*, 16075.

[129] M. E. Byrne, K. Park, N. A. Peppas, *Advanced Drug Delivery Reviews* **2002**, *54*, 149-161.

[130] L. Chen, S. Xu, J. Li, *Recent advances in molecular imprinting technology: Current status, challenges and highlighted applications, Vol. 40*, **2011**.

[131] aC. Malitesta, I. Losito, P. G. Zambonin, *Analytical Chemistry* **1999**, *71*, 1366-1370; bJ. J. BelBruno, *Chemical Reviews* **2019**, *119*, 94-119.

[132] aG. Vasapollo, R. D. Sole, L. Mergola, M. R. Lazzoi, A. Scardino, S. Scorrano, G. Mele, *Int J Mol Sci* **2011**, *12*, 5908-5945; bH. F. El-Sharif, H. Yapati, S. Kalluru, S. M. Reddy, *Acta biomaterialia* **2015**, *28*, 121-127; cY. J. Huang, R. Chang, Q. J. Zhu, *Polymers (Basel)* **2018**, *10*.

[133] K. Mosbach, O. Ramström, *Bio/Technology* **1996**, *14*, 163-170.

[134] L. Chen, X. Wang, W. Lu, X. Wu, J. Li, *Molecular imprinting: Perspectives and applications, Vol. 2016*, **2016**.

[135] A. Uccelli, L. Moretta, V. Pistoia, *Nature Reviews Immunology* **2008**, *8*, 726.

[136] aI. Ullah, R. B. Subbarao, G. J. Rho, *Bioscience reports* **2015**, *35*, e00191; bX. Wei, X. Yang, Z.-p. Han, F.-f. Qu, L. Shao, Y.-f. Shi, *Acta Pharmacologica Sinica* **2013**, *34*,

747; cC. Nombela-Arrieta, J. Ritz, L. E. Silberstein, *Nature Reviews Molecular Cell Biology* **2011**, *12*, 126.

[137] aC. Yang, F. W. DelRio, H. Ma, A. R. Killaars, L. P. Basta, K. A. Kyburz, K. S. Anseth, *Proceedings of the National Academy of Sciences* **2016**, *113*, E4439; bK. M. Schultz, K. A. Kyburz, K. S. Anseth, *Proceedings of the National Academy of Sciences of the United States of America* **2015**, *112*, E3757-E3764.

[138] aM. G. Haugh, T. J. Vaughan, C. M. Madl, R. M. Raftery, L. M. McNamara, F. J. O'Brien, S. C. Heilshorn, *Biomaterials* **2018**, *171*, 23-33; bA. J. Engler, S. Sen, H. L. Sweeney, D. E. Discher, *Cell* **2006**, *126*, 677-689; cA. J. Steward, D. J. Kelly, *J Anat* **2015**, *227*, 717-731; dS. J. Mousavi, M. Hamdy Doweidar, *PLOS ONE* **2015**, *10*, e0124529.

[139] B. Zhang, N. Kasoju, Q. Li, J. Ma, A. Yang, Z. Cui, H. Wang, H. Ye, *Int J Stem Cells* **2019**, *12*, 84-94.

[140] K. Kulangara, K. W. Leong, *Soft Matter* **2009**, *5*, 4072-4076.

[141] S. Sonam, S. R. Sathe, E. K. F. Yim, M. P. Sheetz, C. T. Lim, *Scientific Reports* **2016**, *6*, 20415.

[142] M. Lanniel, E. Huq, S. Allen, L. Buttery, P. M. Williams, M. R. Alexander, *Soft Matter* **2011**, *7*, 6501-6514.

[143] W. L. Murphy, T. C. McDevitt, A. J. Engler, *Nature Materials* **2014**, *13*, 547.

[144] R. Fraioli, P. M. Tsimbouri, L. E. Fisher, A. H. Nobbs, B. Su, S. Neubauer, F. Rechenmacher, H. Kessler, M.-P. Ginebra, M. J. Dalby, J. M. Manero, C. Mas-Moruno, *Scientific Reports* **2017**, *7*, 16363.

[145] Q. Chen, P. Shou, C. Zheng, M. Jiang, G. Cao, Q. Yang, J. Cao, N. Xie, T. Velletri, X. Zhang, C. Xu, L. Zhang, H. Yang, J. Hou, Y. Wang, Y. Shi, *Cell Death And Differentiation* **2016**, *23*, 1128.

[146] J. H. Wen, L. G. Vincent, A. Fuhrmann, Y. S. Choi, K. C. Hribar, H. Taylor-Weiner, S. Chen, A. J. Engler, *Nature Materials* **2014**, *13*, 979.

[147] H. J. Anderson, J. K. Sahoo, R. V. Ulijn, M. J. Dalby, *Frontiers in bioengineering and biotechnology* **2016**, *4*, 38-38.

[148] T. Dvir, B. P. Timko, D. S. Kohane, R. Langer, *Nature nanotechnology* **2010**, *6*, 13.

[149] aK. Dzobo, N. E. Thomford, D. A. Senthebane, H. Shipanga, A. Rowe, C. Dandara, M. Pillay, K. S. C. M. Motaung, *Stem Cells International* **2018**, *2018*, 24; bA. Khademhosseini, R. Langer, *Nature Protocols* **2016**, *11*, 1775; cA. Shafiee, A. Atala, *Annual review of medicine* **2017**, *68*, 29-40.

[150] F. J. O'Brien, *Materials Today* **2011**, *14*, 88-95.

[151] G. Chen, T. Ushida, T. Tateishi, *Macromolecular Bioscience* **2002**, *2*, 67-77.

[152] aA. Eltom, G. Zhong, A. Muhammad, *Advances in Materials Science and Engineering* **2019**, *2019*, 13; bU. Jammalamadaka, K. Tappa, *J Funct Biomater* **2018**, *9*, 22; cP. Rider, Ž. P. Kačarević, S. Alkildani, S. Retnasingh, M. Barbeck, *J Tissue Eng* **2018**, *9*, 2041731418802090-2041731418802090.

[153] aE. Yuksel, J. Choo, M. Wettergreen, M. Liebschner, *Semin Plast Surg* **2005**, *19*, 261-270; bD. Ficai, M. G. Albu, M. Sonmez, A. Ficai, E. Andronescu, in *Nanobiomaterials in Soft Tissue Engineering* (Ed.: A. M. Grumezescu), William Andrew Publishing, **2016**, pp. 355-386.

[154] aN. Kawaguchi, K. Toriyama, E. Nicodemou-Lena, K. Inou, S. Torii, Y. Kitagawa, *Proceedings of the National Academy of Sciences* **1998**, *95*, 1062; bA. Sajjadian, K. Tandav Magge, *Aesthetic surgery journal* **2007**, *27*, 100-104.

[155] aP. Szychta, M. Zadrozny, J. Rykala, L. Banasiak, H. Witmanowski, *Postepy Dermatol Alergol* **2016**, *33*, 323-328; bE. R. Zielins, E. A. Brett, M. T. Longaker, D. C. Wan, *Aesthetic surgery journal* **2016**, *36*, 488-496; cR. A. Agha, T. Goodacre, D. P. Orgill, *BMJ Open* **2013**, *3*, e003709.

[156] E. Stratakis, *Int J Mol Sci* **2018**, *19*, 3960.

[157] A. Tamayol, M. Akbari, N. Annabi, A. Paul, A. Khademhosseini, D. Juncker, *Biotechnol Adv* **2013**, *31*, 669-687.

[158] aT. Garg, *Scaffold: Tissue engineering and regenerative medicine, Vol. 2*, **2011**; bA. S. Mao, D. J. Mooney, *Proceedings of the National Academy of Sciences of the United States of America* **2015**, *112*, 14452-14459; cD. L. Elbert, *Curr Opin Biotechnol* **2011**, *22*, 674-680.

[159] R. Randriantsilefisoa, J. L. Cuellar-Camacho, M. S. Chowdhury, P. Dey, U. Schedler, R. Haag, *Journal of Materials Chemistry B* **2019**, *7*, 3220-3231.

[160] R. Randriantsilefisoa, Y. Hou, Y. Pan, J. L. C. Camacho, M. W. Kulka, J. Zhang, R. Haag, *Advanced Functional Materials* **2019**.

8 Curriculum Vitae

For reasons of data protection, the curriculum vitae is not included in the online version.